University of Cyprus
Department of Biological Sciences

# The HPV16 E6 and E7 oncogenes modify Glutamine metabolism in Cervical Cancers

Vasiliki Andreou

A Research-Based Master's Thesis
for the
Degree of Magister Scientiae in Biomedical Sciences

May 18, 2023

# ABSTRACT

Metabolic reprogramming is an established hallmark of cancer. Malignant cells induce metabolic adjustments to meet their high energy demands and sustain rapid proliferation. These metabolic changes involve modifications in glutamine metabolism including upregulation of transporters and enzymes, and regulation of glutamine uptake by oncogenes and tumor suppressors, to promote glutaminolysis in cancer cells. Cervical cancer continues to pose a significant health burden for women worldwide. Persistent infection with a high-risk Human Papillomavirus (HR-HPV) strain, and subsequent upregulation of the viral oncogenes, E6 and E7, constitute the primary risk factor for the development of cervical cancer. Accumulating evidence supports that the viral oncogenes potentially favor metabolic reprogramming; however, the underlying mechanisms remain unknown. The aim of this research was to investigate whether the oncogenes of HPV16, E6 and E7, promote the rewiring of glutamine metabolism in cervical cancer. To address this, we used the *in vitro* tumor sphere formation assay to assess whether the sphere-forming capabilities of HPV (+) and HPV (-) cervical cancer cells are influenced when glutamine metabolism is hindered or restrained. We found that cervical cancer cells exhibit an impaired ability to form tumor spheres in the absence of glutamine, regardless of HPV presence. Furthermore, transcriptional analysis performed to examine the expression levels of glutamine metabolism-related genes, demonstrated significantly altered expression between HPV (+) and HPV (-) cervical cancer cells. Nevertheless, since we did not identify a consistent expression pattern, we developed a cellular system, where we transduced the HPV (-) C33A cells, to induce expression of E6 and E7, either alone or together, in order to interrogate whether the viral oncogenes are responsible for the differences observed. Transcriptional analysis of C33A-transduced cells revealed that the presence of the E7 oncogene upregulates key genes involved in glutamine metabolism, including the glutamine transporters *Slc1a5* and *Slc7a5*, as well as glutamine metabolism-related enzymes, such as *GLS* and *Glud1*, raising the possibility of facilitated glutamine uptake and increased glutaminolysis in HPV-associated cervical cancers. The consumption of glutamine and glutamate was assessed in oncogene-expressing cells, showing that extracellular glutamine was increased, while extracellular glutamate levels were decreased in the presence of the viral oncogenes, suggesting that E6 and E7, affect the

consumption of these metabolites. Moreover, we demonstrated that the E7-expressing cells are less sensitive to effects of glutamine starvation in the clonogenic potential of cervical cancer cells, since the presence of E7, not only led to an increase in the number of tumor spheres, but also contributed to the growth of larger tumor spheres. Collectively, our data demonstrate the impact of the HPV16 oncogenes, E6 and E7, in promoting metabolic reprogramming through modifying glutamine metabolism to fulfil the high energy requirements of cervical cancer cells, and subsequently support the cancerous phenotype.

# ACKNOWLEDGEMENTS

First and foremost, I would like to express my sincere gratitude to Dr. Katerina Strati, my research supervisor, for providing valuable support and mentorship throughout the completion of my thesis. I have learned a great deal from her expertise and professionalism, and I am grateful for the opportunity to work under her supervision.

Furthermore, I am grateful to my fellow lab members, and especially Dr. Stela Michael, for her constructive feedback and insightful comments, which have greatly contributed to the quality of this thesis.

Finally, I would like to acknowledge the support of my family and friends, who have been a constant source of inspiration, motivation, and love throughout my academic journey. I could not have completed this thesis without their understanding, patience, and encouragement.

# COMPOSITION OF THE EXAMINATION COMMITTEE

Thesis Supervisor (Examination Committee coordinator):

Associate Professor Dr. Katerina Strati

Tumor Viruses and Cancer Laboratory

Department of Biological Sciences, University of Cyprus

Committee Member:

Professor Dr. Antonis Kirmizis

Epigenetics and Gene Regulation Laboratory

Head of the Department of Biological Sciences, University of Cyprus

Committee Member:

Associate Professor Dr. Chrysoula Pitsouli

Drosophila development and Homeostasis Laboratory

Department of Biological Sciences, University of Cyprus

**SEMINAR ANNOUNCEMENT**

University of Cyprus
Department of Biological Sciences

## *Master Research Dissertation in Biomedical Sciences (BIO 830/600)*

# *Student Presentation*

**Thursday, 18 May 2023 at 10:00**

**Building Library, Room LRC014, Panepistimioupoli Campus**

***This seminar is open to the public***

## Vasiliki Andreou

*Thesis Supervisor:* Assoc. Prof. Katerina Strati

## "The HPV16 E6 and E7 oncogenes modify Glutamine metabolism in Cervical Cancers"

Metabolic reprogramming is an established hallmark of cancer. Malignant cells induce metabolic adjustments to meet their high energy demands and sustain rapid proliferation. These metabolic changes involve modifications in glutamine metabolism including upregulation of transporters and

enzymes, and regulation of glutamine uptake by oncogenes and tumor suppressors, to promote glutaminolysis in cancer cells. Cervical cancer continues to pose a significant health burden for women worldwide. Persistent infection with a high-risk Human Papillomavirus (HR-HPV) strain, and subsequent upregulation of the viral oncogenes, E6 and E7, constitute the primary risk factor for the development of cervical cancer. Accumulating evidence supports that the viral oncogenes potentially favor metabolic reprogramming; however, the underlying mechanisms remain unknown. The aim of this research was to investigate whether the oncogenes of HPV16, E6 and E7, promote the rewiring of glutamine metabolism in cervical cancer. To address this, we used the *in vitro* tumor sphere formation assay to assess whether the sphere-forming capabilities of HPV (+) and HPV (-) cervical cancer cells are influenced when glutamine metabolism is hindered or restrained. We found that cervical cancer cells exhibit an impaired ability to form tumor spheres in the absence of glutamine, regardless of HPV presence. Furthermore, transcriptional analysis performed to examine the expression levels of glutamine metabolism-related genes, demonstrated significantly altered expression between HPV (+) and HPV (-) cervical cancer cells. Nevertheless, since we did not identify a consistent expression pattern, we developed a cellular system, where we transduced the HPV (-) C33A cells, to induce expression of E6 and E7, either alone or together, in order to interrogate whether the viral oncogenes are responsible for the differences observed. Transcriptional analysis of C33A-transduced cells revealed that the presence of the E7 oncogene upregulates key genes involved in glutamine metabolism, including the glutamine transporters *Slc1a5* and *Slc7a5*, as well as glutamine metabolism-related enzymes, such as *GLS* and *Glud1*, raising the possibility of facilitated glutamine uptake and increased glutaminolysis in HPV-associated cervical cancers. The consumption of glutamine and glutamate was assessed in oncogene-expressing cells, showing that extracellular glutamine was increased, while extracellular glutamate levels were decreased in the presence of the viral oncogenes, suggesting that E6 and E7, affect the consumption of these metabolites. Moreover, we demonstrated that the E7-expressing cells are less sensitive to effects of glutamine starvation in the clonogenic potential of cervical cancer cells, since the presence of E7, not only led to an increase in the number of tumor spheres, but also contributed to the growth of larger tumor spheres. Collectively, our data demonstrate the impact of the HPV16 oncogenes, E6 and E7, in promoting metabolic reprogramming through modifying glutamine metabolism to fulfil the high energy requirements of cervical cancer cells, and subsequently support the cancerous phenotype.

# TABLE OF CONTENTS

# 1. INTRODUCTION

## 1.1 Cervical Cancer

Cervical cancer is characterized by the growth of malignant cells on the surface of the cervix; the area in the female reproductive system, found between the vagina and the uterus (National Health System 2021). Squamous cell carcinoma and adenocarcinoma are the two predominant types of cervical cancer, with the former accounting for up to 90% of the total cases (National Institute of Health, NIH 2022). Recent epidemiological evidence has shown that cervical cancer is the fourth most frequently diagnosed and the fourth cancer with the highest mortality rates in women worldwide, with most cases occurring in developing countries, due to lack of appropriate screening and prognosis (Arbyn et al. 2020, Bray et al. 2018). According to World Health Organization (WHO), 604.000 women were diagnosed, while 342.000 women died from cervical cancer worldwide, in 2020 (World Health Organization 2022a). Age, smoking, long-term hormonal treatment, as well as Human Papillomavirus (HPV) infection constitute some factors known to increase the risk of cervical carcinogenesis (Zhang, Shaokai et al. 2020). Whereas vaccination against HPV is effective for the prevention of cervical cancer, the lack of access and uptake, complicate the potential of cervical cancer elimination (World Health Organization 2022b).

## 1.2 Human Papillomavirus (HPV)- related Cervical Carcinogenesis

### 1.2.1 Human Papillomaviruses (HPVs)

The main etiological factor for cervical cancer is the infection with a high-risk Human Papillomavirus (HPV) strain. HPVs are small, non-enveloped viruses with a circular, double-stranded DNA genome, with a simple organization. The viral genome is divided into a total of 8 open reading frames (ORFs) coding the early genes (E1, E2, E4, E5, E6, E7), which are necessary for genome replication, and the late genes (L1, L2), that are imperative for viral packaging (Yu et al. 2022) (**Figure 1**).

HPVs are members of the *Papillomaviridae* family. Members included in this family are known to cause genital or skin warts, or can lead to cervical, skin, head and neck, and anogenital

cancers (Bruni L, 2018, Stanley, 2012, zur Hausen, 2009). Although there are approximately 200 HPV types capable of infecting human cells, only some, HPV16 and HPV18, being the most common, are associated with tumorigenesis and so are called “High-Risk”-HPV strains (HR-HPV) (Bouvard et al. 2009). Notably, HR-HPVs are the cause of approximately 5% of all human cancers, with HPV16 to be the most oncogenic type, accounting for the majority of worldwide cervical cancer cases (Ghittoni et al. 2015).

Mucosotropic HPVs are very common viruses, transmitted through sexual contact, and it is known that most sexually active people will be infected at some point of their life (Estêvão et al. 2019). The virus infects the basal layer of squamous epithelia, by gaining access through micro wounds, where it establishes its infection. Nevertheless, ~90% of HPV infections result in viral clearance by the host immune system and only ~10% of cases establish persistent infections and progression to malignancy, suggesting that HPV-induced carcinogenesis is a complex and multistep process (Gupta et al. 2018).

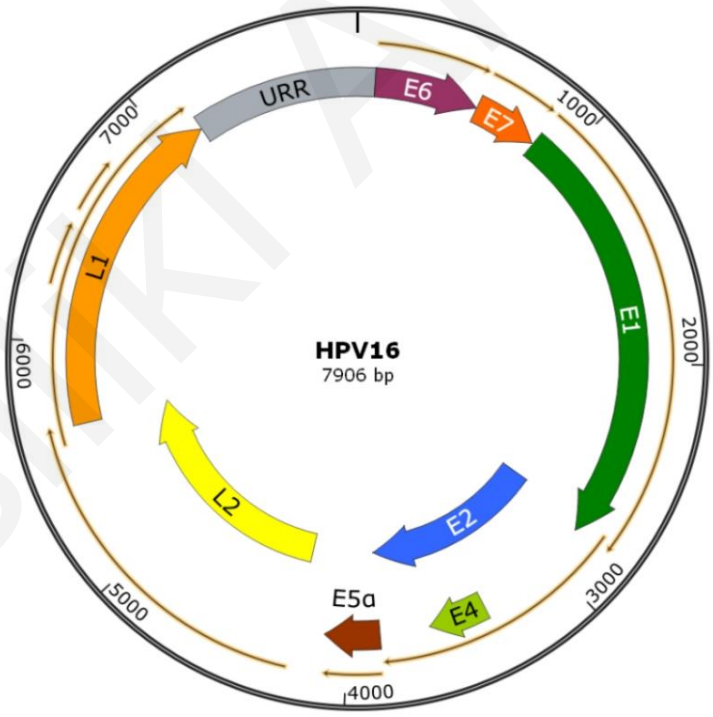


**Figure 1. Schematic representation of the HPV16 viral genome.** The viral genome (7906 base pairs in size) consists of 8 Open Reading Frames (ORFs), encoding the early (E1, E2, E4, E5, E6, E7) and late (L1, L2) genes. Adapted from Neil D. Christensen, 2016 (Neil D. Christensen, 2016).

### 1.2.2 HPV-induced Cervical Carcinogenesis

Cervical carcinogenesis typically arises after accidental integration of the viral genome into the host cell genome and subsequent upregulation of the E6 and E7 oncogenes, due to disruption of E2 functioning to control the transcription of these two oncogenes (Moody, Laimins 2010, Mittal, Banks 2017). HR-HPV E6 and E7 overexpression can promote the malignant transformation of HR-HPV-infected cells during a persistent and long-term infection, mainly by targeting the two major tumor suppressor proteins, p53 (Scheffner et al. 1990, Martinez-Zapien et al. 2016) and pRb (Hwang et al. 2002), respectively, to ubiquitin-dependent proteasomal degradation. In addition, the viral oncogenes can alter signaling pathways, cause genetic instability, and sustain a proliferative signaling, ultimately leading to tumor development and progression (Gupta et al. 2018, Estêvão et al. 2019) gaining the hallmarks of cancer (**Figure 2**) (Hanahan, D., Weinberg 2011, Yang, R. et al. 2019).

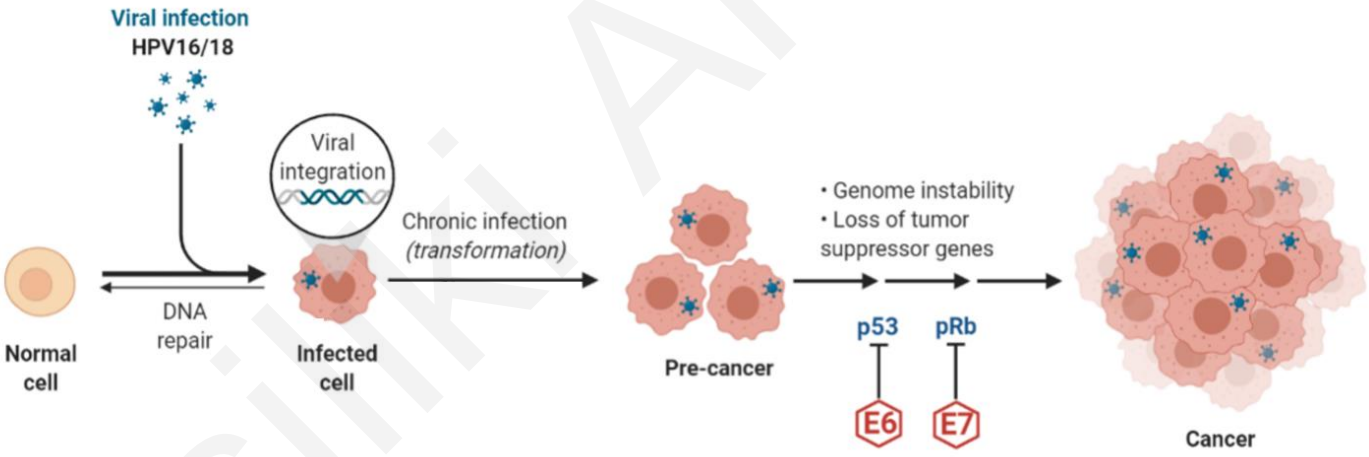


**Figure 2. Simplified model of HPV-induced Carcinogenesis.** Accidental integration of the viral genome into the host cell genome results in upregulation of the viral oncogenes E6 and E7 and progression to malignancy. The figure was created with the use of BioRender.com web application.

### 1.3 Metabolic reprogramming as a Hallmark of Cancer

Metabolic reprogramming has been established as a Hallmark of Cancer (Hanahan, Douglas, Weinberg 2011, Ward, Thompson 2012). Malignant cells, as opposed to normal cells, demonstrate metabolic alterations in order to obtain all necessary nutrients, to fulfill their energy requirements and sustain increased proliferation (Schiliro, Firestein 2021, Martínez-Reyes, Chandel 2021) (**Figure 3**). These deviations in the levels of metabolites can affect gene expression and subsequently the tumor microenvironment (Elia, Haigis 2021). To this end, even though a plethora of various metabolic pathways have been verified to be deregulated upon cancer onset and development, glycolysis has been the most well-known and most extensively investigated up to now (Schiliro, Firestein 2021, Pavlova, Thompson 2016).

Nearly 90 years ago, Otto Warburg demonstrated that cancer cells were remarkably exhibiting elevated glucose consumption compared to normal cells, a phenomenon termed as the "Warburg effect". The Warburg effect states that tumor cells lean towards obtaining their energy by glycolysis and not oxidative phosphorylation, even in scenarios of aerobic conditions, thereby providing them with a major growth advantage, which is more efficient (Pascale et al. 2020, Warburg et al. 1927). Importantly, in addition to glucose metabolism, several other metabolic pathways are altered during the malignant transformation of normal cells, such as the glutamine pathway (Yang, L. et al. 2017).

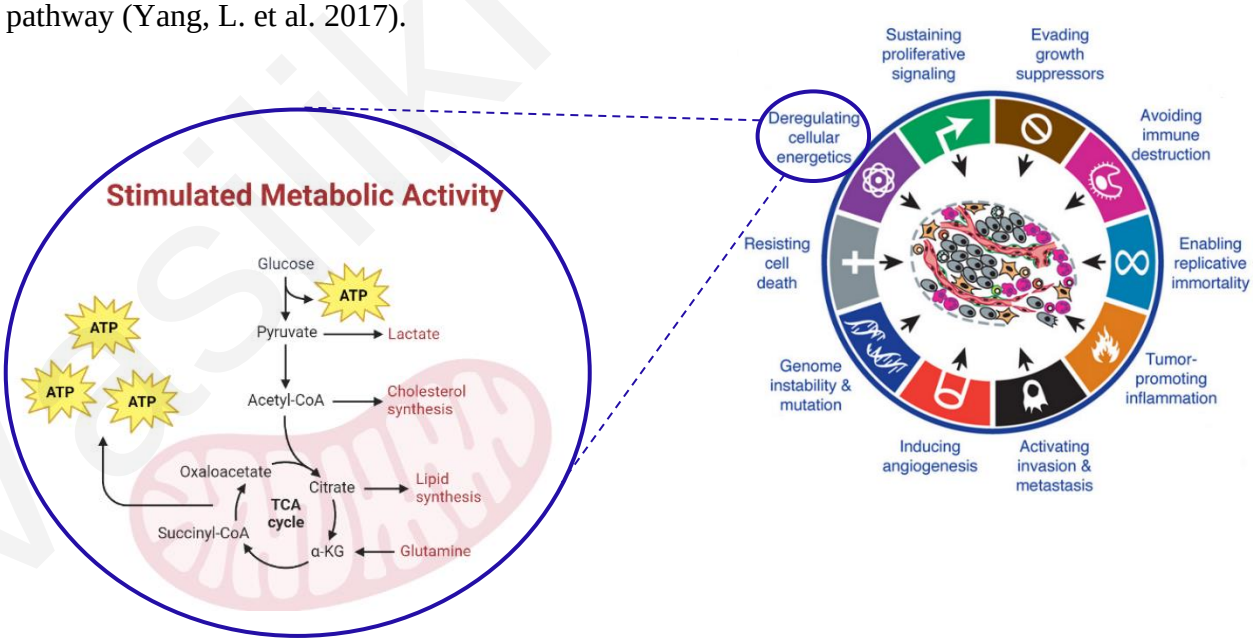

**Figure 3. Metabolic reprogramming as a Hallmark of Cancer.** This illustration summarizes the biological capabilities obtained during the malignant transformation of cells. Deregulation of cellular energetics is the capability of cancer cells to promote metabolic reprogramming to maximize the nutrient intake, fulfill their high energy requirements and sustain increased proliferation. Various metabolic pathways have been reported to be deregulated in cancers, including glycolysis, lipid synthesis, nucleotide synthesis and the glutamine pathway. Adapted from Hanahan, Douglas, Weinberg 2011 (Hanahan, Douglas, Weinberg 2011).

## 1.4 Glutamine Metabolic Pathway and its Role in Cancers

### 1.4.1 Glutamine Pathway

Glutamine is a non-essential amino acid, recognized to be the most abundant in the blood (Li, T., Le 2018). In normal conditions, glutamine enters the cells through transmembrane transporters of the solute carrier (SLC) group, such as the Slc1a5, which is considered the main glutamine transporter. Glutamine uptake in cells is also mediated through other transporters including Slc7a5, Slc7a8 and Slc38a3 (Bhutia, Ganapathy 2016). Upon its entry, glutamine can be converted into glutamate through the catalysis of the glutaminase enzymes, GLS and GLS2. Henceforth, glutamate can be converted into α-ketoglutarate (α-KG) by the glutamine dehydrogenase, GLUD, or the aminotransferase enzymes. α-KG can then enter the tricarboxylic acid (TCA) cycle and provide energy for the cell. Furthermore, glutamate can contribute to the synthesis of glutathione (GSH), mediated by the glutathione synthetase enzyme (GSS). GSH is crucial for the maintenance of redox homeostasis and the regulation of oxidative stress in cells (Yoo et al. 2020) (**Figure 4**).

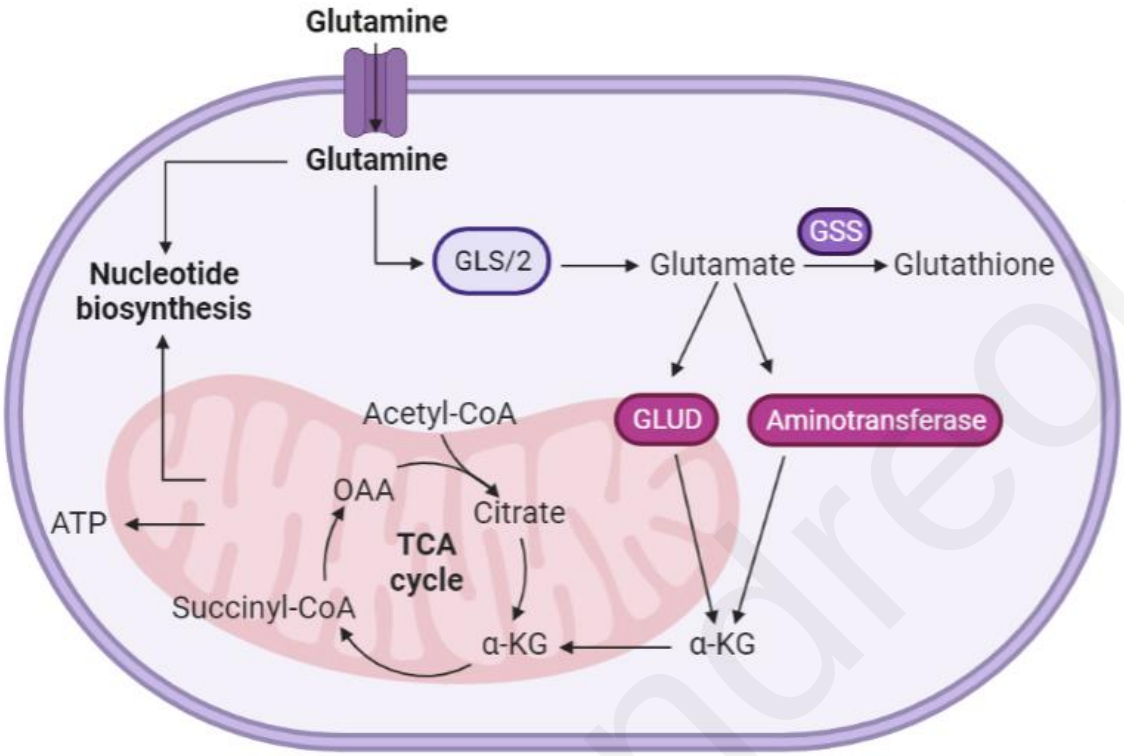


**Figure 4. Glutamine Metabolism Pathway**. Glutamine enters the cells through transmembrane transporters. Glutamine is converted into glutamate by the Glutaminase enzymes, GLS or GLS2. Glutamate can be converted into glutathione by the GSS enzyme, or it can be converted into α-ketoglutarate (α-KG) by the Glutamate Dehydrogenase (GLUD) or aminotransferase enzymes. α-KG enters the TCA cycle and provides energy for the cell. The figure was created with the use of BioRender.com web application.

### 1.4.2 Glutamine Metabolism in Cancers

Glutamine is used by glycolytic cancers for energy production, maintenance of redox balance, biosynthesis of nucleotides and other intermediates, that are necessary for tumor growth (Yoo et al. 2020). Even though it is a non-essential amino acid and can be synthesized *de novo* in the human body, glutamine is an essential carbon and nitrogen donor to sustain high proliferation of cancer cells (Zhang, Ji et al. 2017). Evidence has unveiled that, different types of cancer cells, rely on glutamine to fulfill their energy requirements, while depletion of glutamine results in

cancer cell death (Qie et al. 2012). This phenomenon is commonly referred to as “glutamine addiction”, during which glutamine metabolism is regulated to increase the access of glutamine in cancer cells, while elevated secretion of glutamate is also associated with tumorigenic phenotypes (Wise, Thompson 2010).

Importantly, several studies have demonstrated that to achieve increased glutamine intake, glutamine transporters are deregulated in different cancer types (Bhutia, Ganapathy 2016). For instance, a Pan-cancer analysis performed using data from 9000 patients from The Cancer Genome Atlas (TCGA) dataset, revealed that the main glutamine transporter responsible for controlling glutamine uptake, *Slc1a5*, is found to be upregulated in many human cancers compared to normal tissues, including lung, breast, head and neck, as well as cervical cancer. Moreover, the aforementioned studies have reported that there is an association between *Slc1a5* overexpression in malignant, compared to normal tissues, with poor survival and tumor development, raising the possibility that *Slc1a5* exerts a key role in the process of tumorigenesis (Kanai 2022).

In addition to *Slc1a5*, other glutamine transporters were found to be upregulated in various cancer types, such as *Slc7a5*, *Slc7a8* and *Slc38a3*. The amino acid transporter, *Slc7a5* has been shown to exhibit elevated expression in different types of cancers, including ovarian cancer (OC), non-small cell lung cancer (NSCLC) and breast cancer (BC) (Abd El-Rehim et al. 2005, Kaira et al. 2009, Curtis et al. 2012) , while for the latter, it has been shown to correlate with poor prognosis and survival (Li, Y. et al. 2021) .

Furthermore, *Oncomine* data analysis has revealed, that the expression of *Slc7a8* is augmented in 9 different types of cancers (Wang, Q., Holst 2015), while overexpression of this transporter has been reported to potentially act as a prognostic marker for breast cancer (El Ansari et al. 2020). Additionally, the *Slc38a3* glutamine transporter was also found to be upregulated in NSCLC, as well as in triple negative breast cancer (TNBC). Interestingly, *Slc38a3* was reported to promote epithelial to mesenchymal transition in esophageal cancer (Liu et al. 2020), NSCLC (Wang, Y. et al. 2017) and TNBC (Tan et al. 2021), suggesting the involvement of this transporter in cancer metastasis.

Accumulating evidence shows that glutamine metabolism-related enzymes are also differentially expressed in cancers (Matés et al. 2019). GLS and GLS2, the enzymes converting glutamine into glutamate, as well as GLUD, which converts glutamate into α-KG, are all

exhibiting increased expression in different types of cancers (Jin et al. 2016, Dias et al. 2020, Zhang, Jiannan et al. 2016). Remarkably, even though it is less studied, GSS, the enzyme responsible for the conversion of glutamate into GSH, is also reported to be upregulated in some cancers, such as colorectal cancer (Kim, A. D. et al. 2015).

As mentioned above, malignant cells deregulate glutamine metabolism to increase their glutamine uptake and sustain a high proliferative signalling (Li, T., Le 2018). However, the precise underlying mechanisms that are involved in this process remain unclear. Recent evidence suggests that oncogenes and tumour suppressors can regulate glutamine metabolism, and subsequently glutamine supply. In 2008, Wise et al. revealed that the proto-oncogene, *c-Myc* induces glutaminolysis, the conversion of glutamine into glutamate, by transcriptionally activating *Slc1a5* and *GLS*. Subsequently, this supports increased cellular glutamine uptake and conversion into glutamate, promotion of ATP production from the TCA cycle, resulting in glutamine addiction (Wise et al. 2008, Pavlova, Thompson 2016). Additionally, a study published in *Oncogene* by Reynolds et al., demonstrated that the retinoblastoma (Rb) tumour suppressors control glutamine uptake. They showed that triple knockouts of the Rb family members, *Rb1*, *Rbl1* and *Rbl2*, resulted in elevated glutamine uptake and conversion into glutamate, through upregulation of the *Slc1a5* and *GLS*, which is mediated by E2F (Reynolds et al. 2014). Overall, the findings of these studies suggest that oncogenes and tumour suppressors can modify glutamine metabolism by allowing increased access of glutamine in cancer cells, enabling their uncontrolled proliferation (Ni et al. 2023, Kim, M. H., Kim 2013, Pavlova, Thompson 2016).

## 1.5 Aim of study

In HPV-positive cervical cancers, the viral oncogenes, E6 and E7 promote and preserve carcinogenesis, through various mechanisms (Mittal, Banks 2017). Remarkably, it has been reported that the HR-HPV oncogenes potentially favor metabolic reprogramming by modifying glucose, lipid, and glutamine metabolism, with the underlying mechanisms to remain elusive (Arizmendi-Izazaga et al. 2021, Li, B., Sui 2021, Pappa et al. 2021). Nevertheless, the limited evidence regarding the effect of the HPV16 E6 and E7 oncogenes on glutamine metabolism in cervical cancers provides space for further investigation.

Preliminary data arising from a functional enrichment analysis that we have conducted, using as an input the transcriptome data, comparing cells expressing the viral oncogenes or not revealed pathways and gene ontology terms related to glutamine metabolism. The outcomes of this analysis led us to hypothesize that the viral oncogenes may exert a potential impact on glutamine metabolism in cervical cancers.

**The aim of this study was to examine the potential effects of the HPV16 E6 and E7 oncogenes on glutamine metabolism in cervical cancers.**

To address this, we divided our aim into 3 sub-aims:

**Aim 1: Investigate the functional implications of glutamine metabolism in HPV-mediated carcinogenesis.** To pursue this aim we evaluated the effects of glutamine on the clonogenic potential of HPV (+) and HPV (-) cervical cancer cell lines, using different concentrations of L-glutamine, including glutamine starvation.

**Aim 2: Identify the transcriptional differences of glutamine transporters and glutamine metabolism-related enzymes in HPV (+) and HPV (-) cervical cancers.** To address this, we performed RT-PCR analysis to check whether the expression of E6 and E7 affects the expression levels of glutamine metabolism-related genes in cervical cancer cells.

**Aim 3: Investigate the alterations on the functionality of glutamine metabolism in HPV-expressing cervical cancers**. To accomplish this, we assessed the levels of metabolites involved in glutamine pathway in cervical cancers expressing the viral oncogenes E6 and E7.

# 2. MATERIALS AND METHODS

## 2.1 Cell culture

Cervical cancer cell lines, HeLa (HPV18), Caski (HPV16) and C33A (HPV-negative) were purchased from American Type Culture Collection (ATCC). HeLa and Caski cells were cultured in Dulbecco's Modified Eagle Medium (DMEM) and Roswell Park Memorial Institute (RPMI) respectively, while C33A cells were cultured in Minimum Essential Media (MEM) supplemented with 1% L-glutamine. The 293T human epithelial kidney cells, purchased also from ATCC, were cultured in DMEM. All cell culture media were supplemented with 1% penicillin-streptomycin (penstrep) and 10% fetal bovine serum (FBS) (Invitrogen). All cell culture media were purchased from Invitrogen. Cells were grown in a humidified atmosphere at 37℃ containing 5% $CO_2$. All cell lines were routinely tested for mycoplasma contamination.

## 2.2 Plasmid DNA purification from bacterial cultures

After the overnight incubation (12-18h) of liquid bacterial cultures containing LB (Luria Broth) and the different plasmids of interest (**Table 1**) at 37℃ in a shaking incubator, the DNA was purified using the Midi prep DNA purification kit from Qiagen (12143). Harvesting of the bacterial culture was done by centrifuging at 6000 x *g* for 15 minutes at 4℃. After resuspension of the bacterial pellet in alkaline lysate, the supernatant was passed through columns to bind the DNA, followed by washes to clean the columns. To elute DNA, elution buffer was added to the columns. DNA precipitation was achieved by adding isopropanol (at room temperature) to the eluted DNA, followed by centrifugation at >15,000 x *g* for 30 minutes at 4℃. The supernatant was then decanted, and the DNA pellet was washed with room temperature 70% ethanol, followed by centrifugation at >15,000 x *g* for 10 minutes. After decanting the supernatant, the pellet was air-dried for 5-10 minutes. DNA is redissolved in TE buffer, pH 8.0.

## 2.3 Transfections- Retroviral transduction

293T cells were plated at a density $1x10^6$, in 10cm tissue culture plates, containing DMEM and incubated at 37℃, 5% $CO_2$. 24 hours later, seeded cells were co-transfected with the plasmids mentioned in **Table 1**. The transfection of 293T cells was performed using the Fugene transfection reagent (Promega) at a ratio 1:3 (Fugene to DNA). For the transduction experiments, $1x10^5$ C33A cells were seeded in 6-well plates. 48 hours post-transfection the retroviral constructs were collected from 293T cells, filtered using 0.45μm filter, and applied to C33A with 1μg/ml Polybrene (Sigma) (1:1000 ratio). 293T cells were replenished with DMEM to further collect the virus at day 5 and 6 post-transfection. The virus collected at day 5 was filtered and stored in -80℃ to be used for further experiments, while the medium containing the retrovirus collected at day 6, was used to perform the 2nd transduction. 48 hours after the second transduction, the virus was removed from C33A cells and MEM containing geneticin (G418) (GIBCO) was added at 1:1000 ratio, to select for the cells expressing the gene of interest. Geneticin was applied in C33A cells every 48 hours (**Figure 5**).

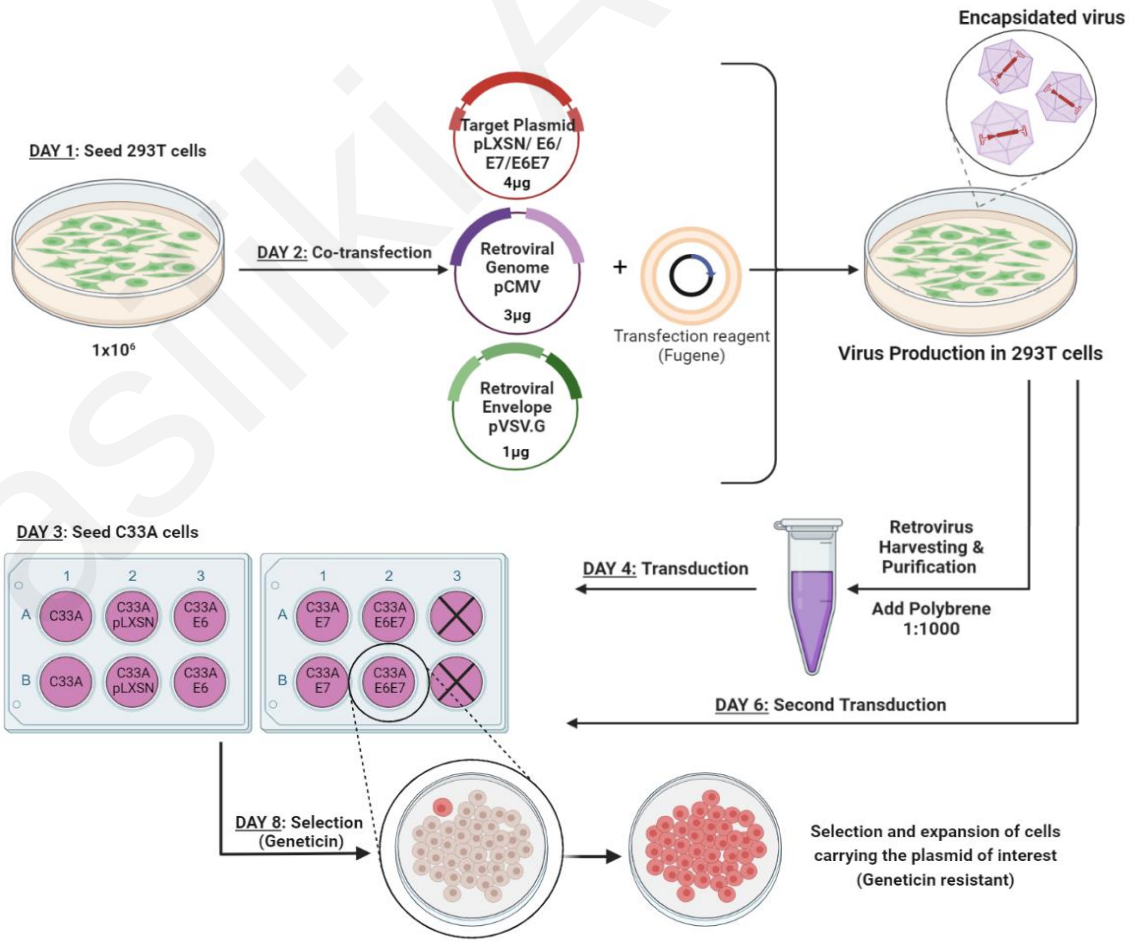

**Figure 5. Graphical illustration of the procedure followed for the transfection/ transduction experiment performed using the HPV-negative (-) cervical cancer cell line C33A.** 293Ts are used for viral production. 24-hours post- seeding, 293Ts are co-transfected, using Fugene as the transfection reagent, with the plasmids expressing the target gene (pLXSN, E6, E7 or E6E7) and the retroviral genome and envelope. The target cells, C33A, are seeded at day 3. 48-hours post-transfection, the formed retroviral particles are harvested and filtered, followed by transduction in C33A cells. A second transduction is performed at day 6. 48-hours post the second transduction, the virus is removed from the C33A cells and the medium, containing Geneticin, is replenished. C33A cells expressing the genes of interest are resistant to Geneticin and are expanding. The figure was created with the use of BioRender.com web application.

**Table 1. List of plasmids used for the transfection/transduction experiments.**

| Plasmid | Company | Type | Selection |
|---|---|---|---|
| **pLXSN empty** | Addgene | Retroviral | Geneticin (G418) 1:100 |
| **pLXSN 16E6** | Addgene | Retroviral | Geneticin (G418) 1:100 |
| **pLXSN 16E7** | Addgene | Retroviral | Geneticin (G418) 1:100 |
| **pLXSN 16E6E7** | Addgene | Retroviral | Geneticin (G418) 1:100 |
| **pUMVC Packaging** | Addgene | Retroviral | Geneticin (G418) 1:100 |
| **VSV.G envelop** | Addgene | Retroviral | Geneticin (G418) 1:100 |

## 2.4 Polymerase Chain Reaction (PCR) and Agarose Gel Electrophoresis

Polymerase Chain Reaction (PCR) was performed to assess the transduction efficiency of the C33A cells, using the KAPA Taq PCR kit (KK1016) (Kapa Biosystems), as per manufacturer's

instructions. Primers for HPV16 E6 and HPV16 E7 were used, while GAPDH was used as the loading control. Primers were purchased from Integrated DNA Technologies, Inc. (IDT). The primer sequences used for PCR and their annealing temperatures are listed in **Table 2.** The end-result of the PCR was loaded on 1.5% DNA agarose gel (30mL Tris-Acetate-EDTA (TAE), 45gr agarose) and visualized under an ultraviolet (UV) lamp, using the G-box (SYNGENE).

### 2.5 RNA extraction from cells

Total RNA was purified from cells using the QIAGEN's RNeasy Mini Kit (74106) according to the manufacturer's instructions, under RNAse free conditions. Briefly, cells were lysed and homogenized in the presence of a highly denaturing guanidine-thiocyanate-containing buffer (RLT Buffer) mixed with β-mercaptoethanol, which ensures the purification of intact RNA by immediately inactivating RNAses. Ethanol was then added to the lysate to create the appropriate binding conditions that promote the selective binding of RNA to the RNeasy membrane on the RNeasy Mini spin column. After centrifugation for 15 seconds at >8000 x *g*, DNase was added on the RNeasy Mini spin column, followed by incubation for 15 minutes at room temperature, to digest every DNA molecule bound on the RNeasy membrane. Total RNA binds to the membrane and contaminants were efficiently washed away after the addition of washing buffers (RW1 & RPE buffer). High-quality RNA was eluted in RNAse free-water solution. All the steps were performed by centrifugation in a microcentrifuge at >8000 x *g*. The concentration of the RNA was measured using a NanoDrop 2000 Spectrophotometer (ThermoFisher Scientific).

### 2.6 cDNA synthesis

Using the iScript™ cDNA Synthesis Kit (BIORAD), 500ng RNA from each sample was converted into cDNA. A master mix of 4μL 5x iScript Reaction Mix, which contains oligo(dT) and random hexamers and 1μL of iScript Reverse Transcriptase, was prepared. In each PCR tube, the amount of the RNA template and water that was added was variable according to the concentration of the RNA sample. Total volume of the reaction was 20μL. Amplification of cDNA was achieved by performing PCR reactions using the KAPATaq (KapaBiosystems)

standard PCR protocol. For the characterization of the C33A-transduced tumor spheres, since the RNA concentration was low for some samples, cDNA synthesis was performed using the NEBNext® Single Cell/Low Input cDNA Synthesis & Amplification Module (E6421S), according to manufacturer's instructions.

### 2.7 Gene Expression Analysis

Quantitative Real Time–PCR (qPCR) was performed using KAPA SYBR FAST qPCR Master Mix (2X) kit from Kapa Biosystems in a BIORAD CFX96 Real-Time system. One µL of cDNA was added to each PCR reaction (10 µL), containing 0.5 µL of each primer and 5 µL of 2X iTaq SYBR Green super mix. Primer pairs were designed using the Primer3Plus software and were purchased from Integrated DNA Technologies, Inc. (IDT). The primer sequences used for Real-Time PCR and their annealing temperatures are listed in **Table 2**. For input normalization the housekeeping gene Actin was used, unless otherwise stated in the figure legend. The protocol used is represented in **Figure 6**.

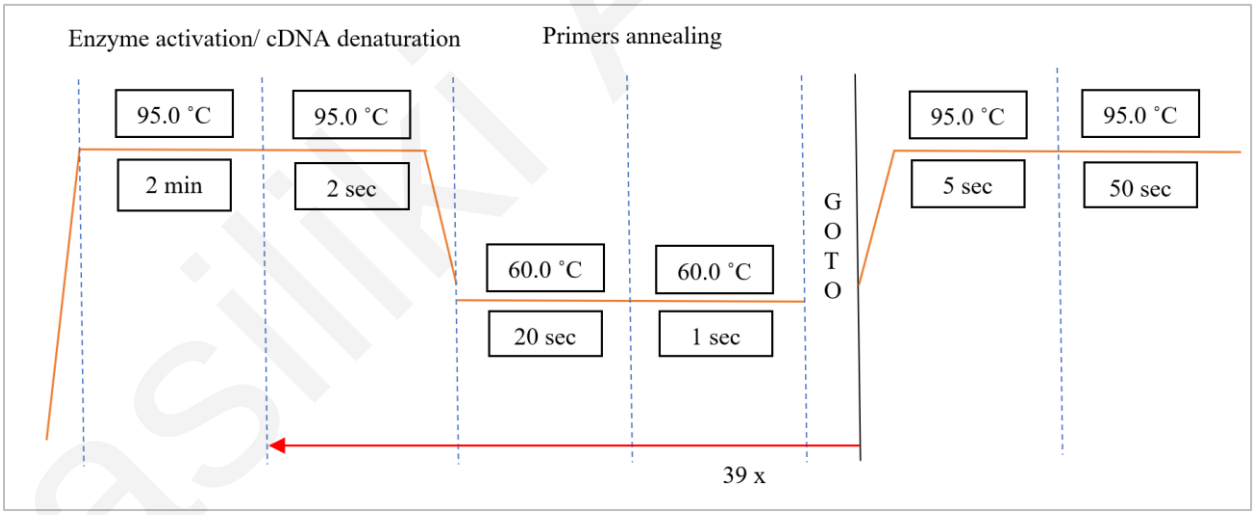


**Figure 6. Schematic representation of the RT-qPCR thermal profile.** Firstly, high temperature (95°C) is required to activate the DNA polymerase and denature the double-stranded cDNA. Following denaturation, the temperature decreases (60°C) to allow the primers to hybridize with the single strands of the cDNA and start the amplification of the target gene. This process is repeated for 39 cycles.

### 2.8 Glutamine- Glutamate consumption assay

Transduced C33A cells, C33A-pLXSN, C33A HPV16 E6, C33A HPV16 E7 and C33A HPV16 E6E7, were plated at 20,000 cells/well in 96-well plates in MEM supplemented with 1% L-glutamine, 1% Penicillin-Streptomycin and 10% FBS. After 72 hours of incubation, the medium was removed, and cells were washed twice with PBS, to ensure the removal of glutamine and exclude possible cross contaminations. Next, cells were starved for two and a half hours in MEM medium without glutamine. After that, MEM medium supplemented with 2mM of glutamine was replenished in cells for 30 minutes to allow glutamine consumption. Cell culture medium of each condition was diluted in PBS (1:20 dilution). Two 25μL aliquots were transferred to a 96-well plate for the assay. 25μL of Glutaminase was added in the Glutaminase Buffer and added to the wells that would be used to measure total glutamine and glutamate levels, while 25μL of Glutaminase Buffer (no Glutaminase) was added to the wells used to measure glutamate only levels, followed by incubation for 40 minutes at room temperature. After the incubation, 50μL of Glutamate Detection Reagent (containing 50μL Luciferin Detection Solution, 0.25μL Reductase and 0.25μL Reductase Substrate, 1μL Glutamate Dehydrogenase and 1μL NAD) was added to all wells, followed by 1 hour incubation at room temperature and plate-reading using the TECAN Spark Multimode multiplate reader, to measure luminescence and quantify the levels of glutamine and glutamate in the cell culture medium.

### 2.9 Tumor sphere formation assay

To assess the clonogenic potential and the ability of cervical cancer cells to self-renew in different concentrations of L-glutamine, ultra-low attachment 6-well plates (Corning) were used for the seeding of $1x10^3$ cells/well. C33A, Caski and HeLa cervical cancer cells, as well as C33A-transduced cells (pLXSN, E6, E7, E6E7) were used for these experiments. The cells were incubated for 10 days with DMEM/F12 (Invitrogen) combined with B27 supplement (GIBCO), 20 ng/ml basic FGF (Fibroblast Growth Factor) (Invitrogen), 20 ng/ml EGF (Epidermal Growth Factor) (Invitrogen) and 1%, 0.5% and 0% L-glutamine, in 37°C and 5% $CO_2$. 200μL of medium was added every two days. The tumor spheres formed were viewed and counted manually under the microscope (Zeiss Axio Observer.A1). The data of this analysis were plotted using the

GraphPad Prism software. The diameter of tumor spheres was calculated by the AxioVision software, while the plots were created using the PowerPoint. All clones with diameter equal or more than 100μm were considered as tumor spheres. The procedure of the *in vitro* tumor spheres assay is summarised in **Figure 7**.

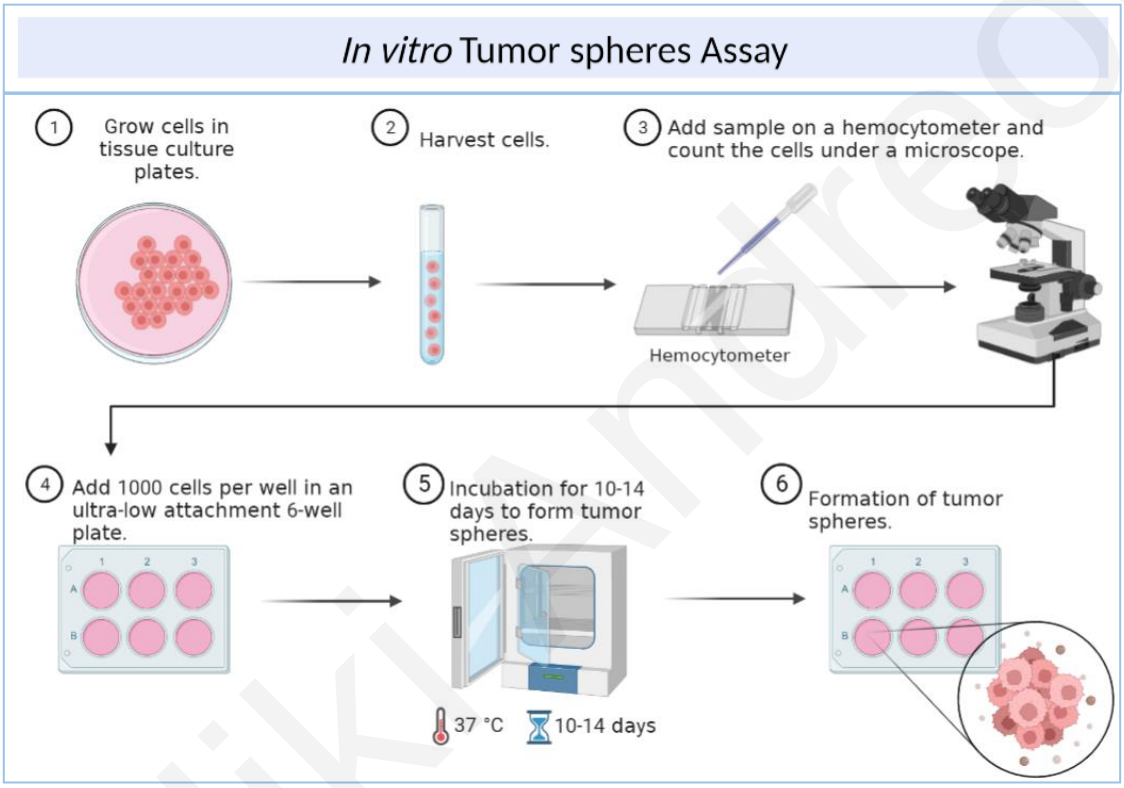


**Figure 7. Graphical representation outlining the methodology followed for the *in vitro* tumor sphere formation assay**. The cells to be used for the assay are cultured in tissue culture plates until they are fully confluent, harvested and counted. 1000 cells per well are added in ultra-low attachment 6-well plates, followed by incubation for 10 days in 37°C and 5% $CO_2$, to form tumor spheres. The figure was created with the use of BioRender.com web application.

## 2.10 Imaging

For the visualization of cells and tumor spheres, the Zeiss Axio Observer.A1 microscope was used. The microscopy images were taken with the Axio camera using the 10X lens. To count the

tumor spheres formed at day 10 of the tumor sphere assay, a specific area of the well was defined (**Figure 8**). The diameter size was determined for 20 tumor spheres in each well. For the quantification and measurements of the tumor spheres diameter, the AxioVision software was used.

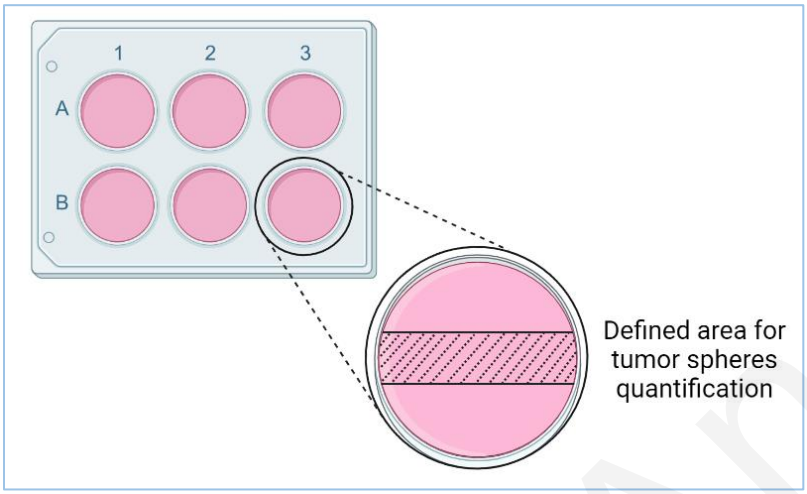


**Figure 8. Schematic representation of the area that was defined for the quantification of the tumor spheres.** The area of the 6-well that was defined for the quantification is illustrated with diagonal, parallel lines. The figure was created with the use of BioRender.com web application.

### 2.11 Statistical methods

Statistical analyses of the data were performed using GraphPad Prism v.8.0.1 (La Jolla, CA). Differences between groups were analyzed using the one-way ANOVA statistical test for multiple comparisons. Data represent the mean ± SEM (Standard Error of the Mean). For each gene in Real-Time PCR, the average C(t) value was determined and normalized to mRNA levels of the housekeeping gene, *Actin*, unless otherwise stated in the figure legend. All the experiments were performed using three independent biological replicates and three technical replicates. A *P*-value of $< 0.05$ was considered statistically significant.

**Table 2. Sequences of Primer sets used in the study.** The table depicts the primer sequences (forward and reverse), as well as the annealing temperature for each primer set.

| | Primers | Forward Primer (5'→ 3') | Reverse Primer (5'→ 3') | Annealing Temp. (°C) |
|---|---|---|---|---|
| 1 | ***Slc1a5*** | TCTTTTTCCTGGTCACCACGCT | CTGACACCAGGTTGGAAGGGA | 60 |
| 2 | ***Slc7a5*** | TCATCATCCGGCCTTCATCG | TCACGCTGTAGCAGTTCACG | 60 |
| 3 | ***Slc38a3*** | GAGCGCCGCACGTTCCC | GTGTTTGCCATTGGGCACCAG | 60 |
| 4 | ***Slc7a8*** | CCAGGCACCGAAACAACACC | TCTCCAGCACTCCCTTTGGC | 60 |
| 5 | ***GLS*** | GGAAGCCTGCAAAGTAAACCC | CCAAAGTGCAGTGCTTCATCC | 60 |
| 6 | ***GLS2*** | AGAGAGACGCCACACAGCCA | CAGTGGCCTTTAGTGCAGTGG | 60 |
| 7 | ***GSS*** | AACCGTTCGCGGAGGAAAGG | GCATAGCTCACCACCTCCGA | 60 |
| 8 | ***GLUD1*** | CTAGTCGCGGGGAGTCTGAG | GTACATGGCCACAAGCGGAG | 60 |
| 9 | ***Oct4*** | CAAGGGCCGCAGCTTACACATGTT | CGTGAAGCTGGAGAAGGAGAAGCT | 60 |
| 10 | ***Sox2*** | CGCCCCCAGCAGACTTCACA | CTCCTCTTTTGCACCCCTCCCATTT | 60 |
| 11 | ***Klf4*** | GAAATTCGCCCGCTCAGATGAACT | TCTTCATGTGTAAGGCGAGGTGGT | 60 |
| 12 | ***Nanog*** | AGTCCCAAAGGCAAACAACCCACTTC | ATCTGCTGGAGGCTGAGGTATTTCTGTCTC | 60 |
| 13 | ***HPV16 E6*** | AGCAATACAACAAACAGTTGTGT | CCGGTCCACCGACCCCTTAT | 56 |
| 14 | ***HPV16 E7*** | ATGGAGATACACCTACATTGCATGA | AATGGGCTCTGTCCGGTTCT | 56 |
| 15 | ***Actin*** | CGAGCACAGAGCCTCGCCTTT | TGTCGACGACGAGCGCGGGG | 60 |
| 16 | ***GAPDH*** | TGCACCACCAACTGCTTAGC | GGCATGGACTGTGGTCATGAG | 60 |
| 17 | ***B2M*** | CCACTGAAAAAGATGAGTATGCCT | CCAATCCAAATGCGGCATCTTCA | 60 |
| 18 | ***Nono*** | CATCAAGGAGGCTCGTGAGAAG | TGGTTGTGCAGCTCTTCCATCC | 60 |
| 19 | ***Mycoplasma*** | ACACCATGGGAGYTGGTAAT | CTTCTCGACTTCAGACCCAAGGCAT | 60 |

# 3. RESULTS

**Our aim in the current study was to assess whether the viral oncogenes, E6 and E7, influence glutamine metabolism in cervical cancers.** To dissect this, HPV (+) and HPV (-), as well as E6/E7-transduced HPV (-) cervical cancer cells were used to interrogate the functional implications of glutamine metabolism in HPV-mediated carcinogenesis, discover potential differences in expression of key genes involved in glutamine pathway, and examine whether there are evident alterations in the functionality of glutamine metabolism in the presence or absence of E6 and E7.

## 3.1 Glutamine starvation reduces the sphere-forming ability of cervical cancer cells

To assess whether the clonogenic potential of cervical cancer cells is affected in decreased levels or completely devoid of glutamine, in the presence or absence of the viral oncogenes, E6 and E7, we used the HPV-negative, C33A, and the HPV-positive cervical cancer cell lines, HeLa (HPV18-positive) and CaSki (HPV16-positive), to perform the *in vitro* tumor sphere formation assay in different concentrations of L-glutamine (1%, 0.5% and 0% L-glutamine). On day 5 (**Appendix 1**) and day 10 (**Figure 9**) of the assay, representative images were captured for all three different cell lines and conditions that were tested. As illustrated in **Figure 9**, at day 10 of the tumor sphere assay, there were no significant differences in number, or size, of the tumor spheres formed in the reduced 0.5% L-glutamine concentration and the 1% L-glutamine control concentration, for all the three cell lines. Interestingly, in glutamine starvation (0% L-glutamine), we observed fewer and smaller tumor spheres, compared to the control, in all different cervical cancer cell lines, expressing or not the viral oncogenes. This result suggests that cervical cancer cells demonstrate an impaired ability to form tumor spheres in the absence of L-glutamine.

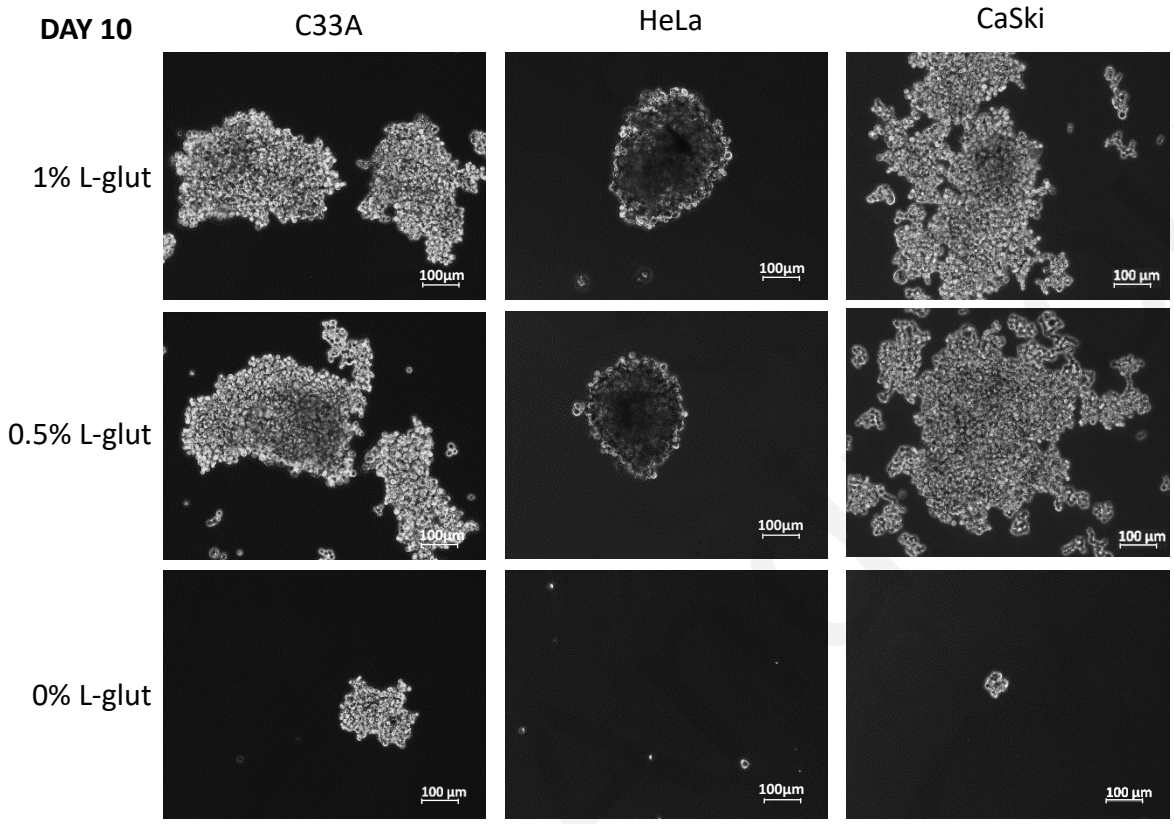


**Figure 9. Glutamine starvation reduces the sphere-forming capacity of cervical cancer cells.** Representative phase-contrast images of the tumor spheres formed in the cervical cancer cells C33A, HeLa and CaSki, in different concentrations of L-glutamine (1%, 0.5% and 0% L-glutamine). The images were taken on day 10 of the tumor spheres assay, using the 10x lens of the Axio camera (Zeiss Axio Observer.A1) and are representative of three independent experiments. Scale bars, 100µm.

## 3.2 Enrichment of stemness-related genes in tumor spheres formed from cervical cancer cell lines

It is widely appreciated that tumor spheres are enriched for the presence of cells with Cancer Stem Cell (CSCs) activity, and often demonstrate increased expression of stemness markers, such as *Oct4*, *Sox2*, *Klf4*, etc. (Tirino et al. 2013). To elucidate whether that is indeed the case for

our tumor spheres formed from the cervical cancer cells C33A, HeLa and CaSki, we performed RT-qPCR to quantify the expression of some stemness markers. The results of this analysis demonstrated that all stemness markers tested, including *Oct4*, *Sox2*, *Klf4* and *Nanog* were significantly enriched in tumor spheres formed in all different glutamine concentrations (1%, 0.5% and 0% L-glutamine), compared to the adherent C33A, HeLa, and CaSki cervical cancer cells. C33A tumor spheres formed in all different glutamine concentrations, demonstrated enhanced expression of all stemness markers, compared to the adherent C33A cells. Interestingly, the most significant upregulation was observed in C33A tumor spheres formed in the 0% L-glutamine concentration (**Figure 10A**). Additionally, the expression of all stemness markers was increased in HeLa tumor spheres (1%, 0.5% and 0% L-glutamine), compared to the adherent HeLa cells, yet the upregulation was only statistically significant in tumor spheres formed in 0% L-glutamine (**Figure 10B**). Moreover, upregulation of all stemness genes was also observed in CaSki tumor spheres, compared to the adherent cells. However, this difference was statistically significant in tumor spheres formed in 0.5% and 0% L-glutamine concentrations, with the 0% showing the most significant upregulation for all stemness markers, except for *Klf4* (**Figure 10C**).

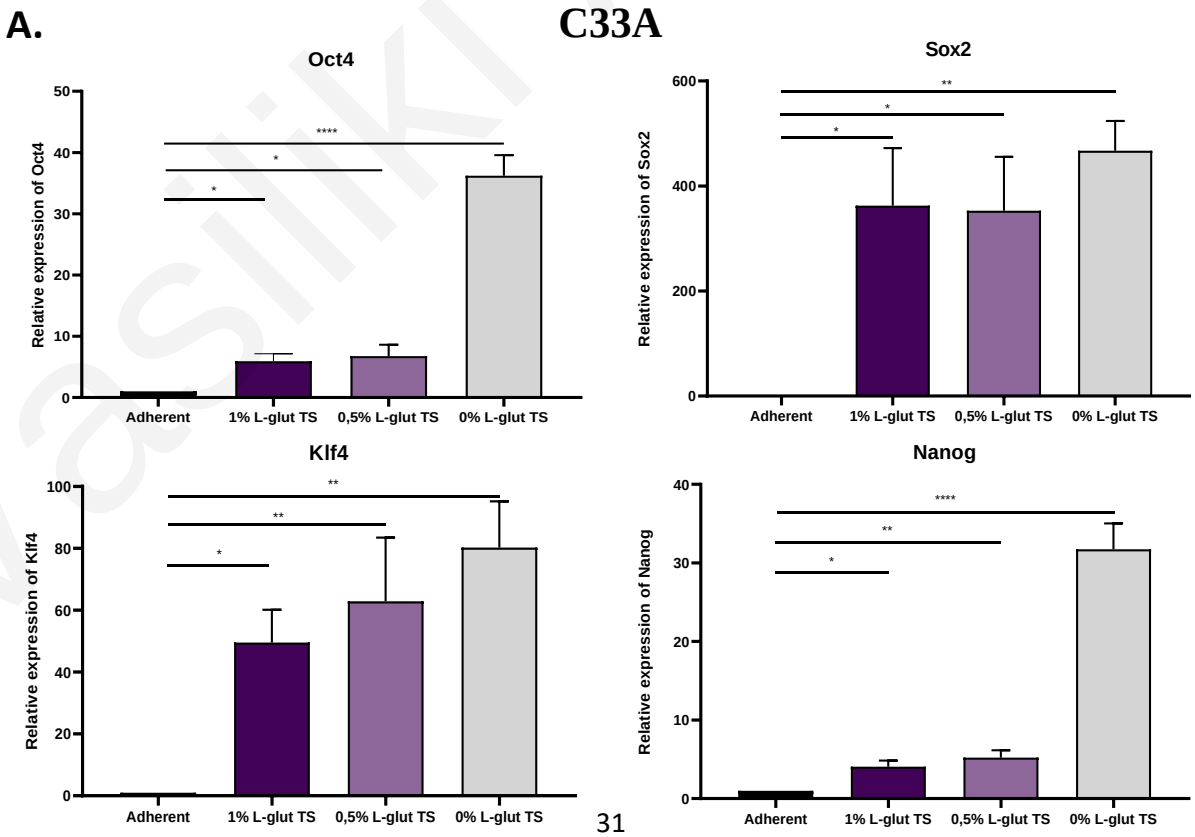

**B.** **HeLa**

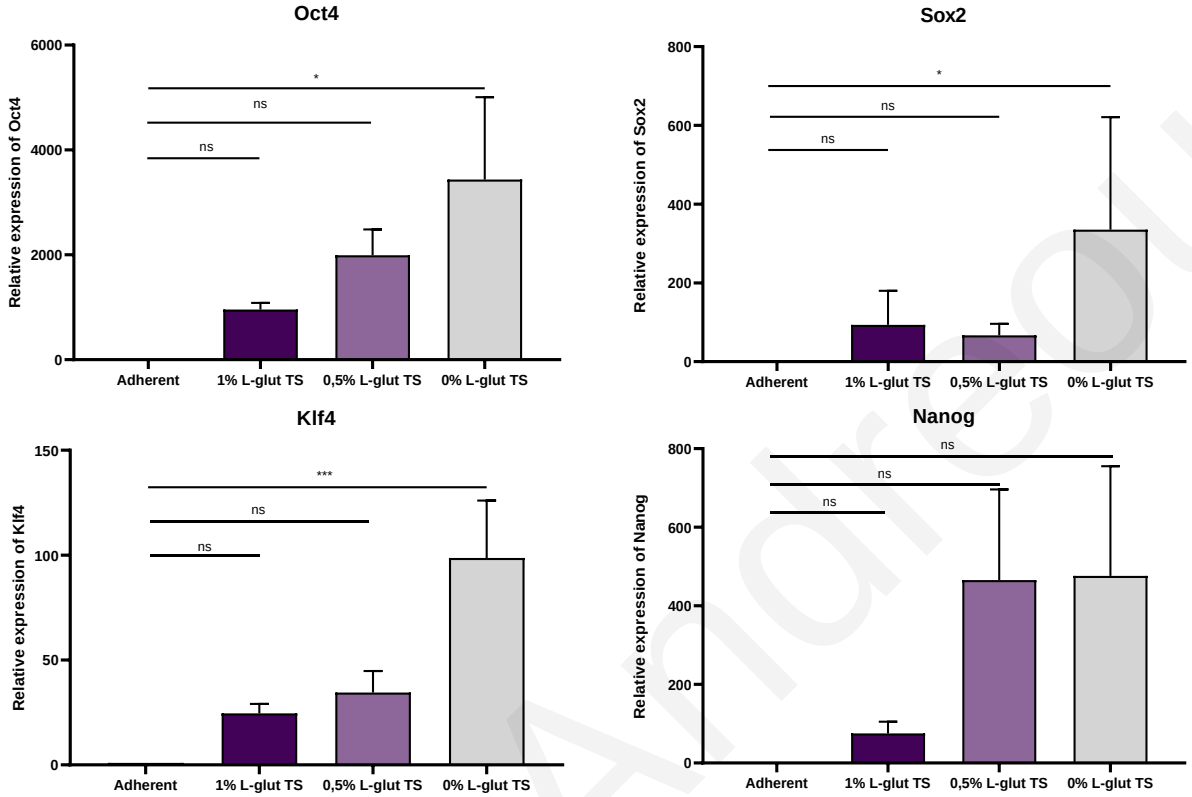


**C.** **CaSki**

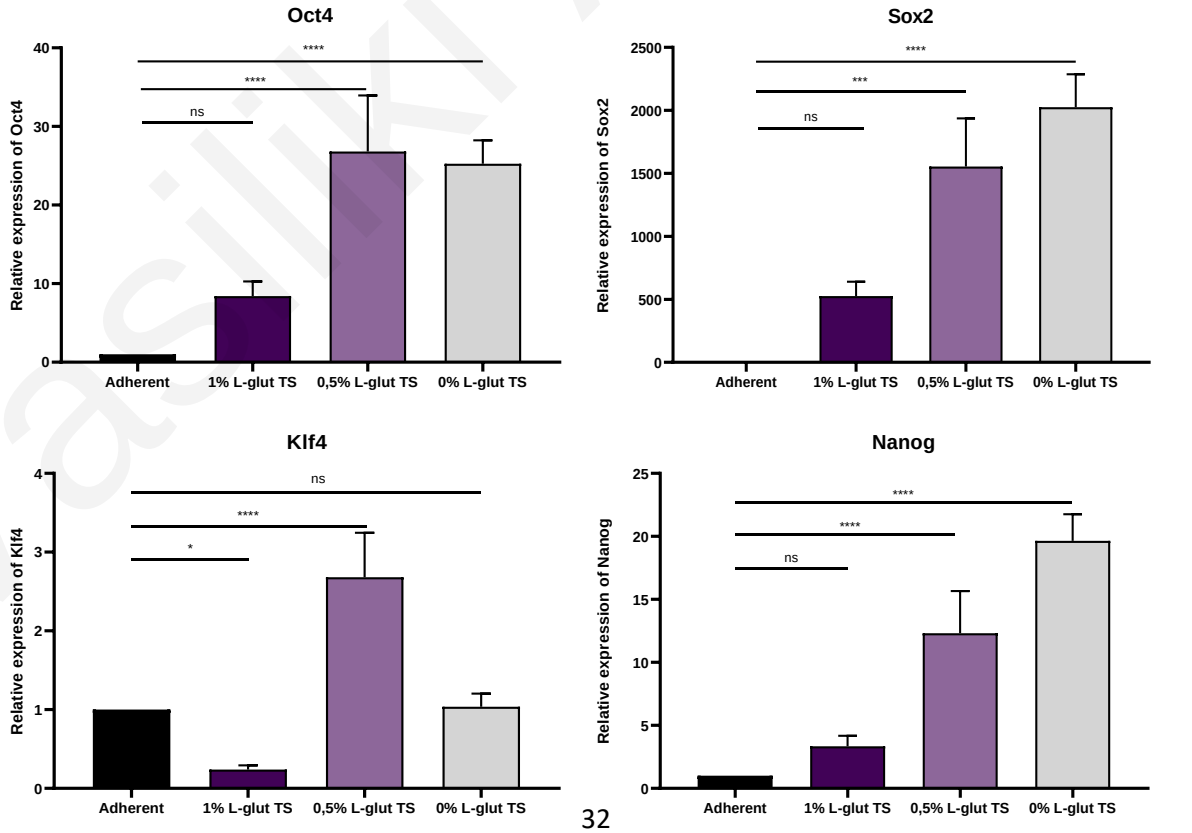

**Figure 10. Enrichment of stemness-related genes in tumor spheres formed from Cervical cancer cell lines.** RT-qPCR was performed to examine the expression of stemness genes Oct4, Sox2, Klf4, and Nanog, in the tumor sphere populations formed in different concentrations of L-glutamine (1%, 0.5%, 0% L-glutamine) compared to the adherent cervical cancer cells, **(A)** C33A, **(B)** HeLa and **(C)** CaSki. *Actin* expression was used for normalization. Data presented as mean ± SEM of three biological replicates and are representative of three independent experiments. Statistical significance was evaluated using the one-way ANOVA statistical test. P <0.05 was considered statistically significant. (ns = non-significant, *p<0.05, **p<0.01, ***p<0.001, ****p<0.0001).

### 3.3 Glutamine transporter, *Slc1a5*, and glutaminase enzyme, *GLS*, expression is deregulated in tumor spheres derived from cervical cancer cells in reduced glutamine concentrations

The glutamine transporter, *Slc1a5* and the glutaminase enzyme, *GLS* are the main glutamine metabolism-related genes reported to be deregulated in cancers (Bhutia, Ganapathy 2016). To investigate whether the expression of these key genes is affected in tumor spheres formed from the cervical cancer cell lines C33A, HeLa and CaSki, in different concentrations of L-glutamine (1%, 0.5% and 0% L-glutamine), RT-qPCR analysis was performed. Our results demonstrated that in C33A and CaSki tumor spheres, *Slc1a5* was significantly downregulated in 0.5% and 0% L-glutamine concentrations, compared to the control. On the contrary, HeLa tumor spheres exhibited significant upregulation of *Slc1a5*, only in the 0% L-glutamine concentration, compared to the control (**Figure 11A**). Furthermore, *GLS* displayed enhanced expression in the 0.5% and 0% L-glutamine concentrations, in C33A, as well as in CaSki tumor spheres, compared to the control, while demonstrated increased expression in HeLa tumor spheres formed in 0.5% and 0% L-glutamine concentrations, compared to the control, however the result was not statistically significant (**Figure 11B**). This suggests that glutamine metabolism-related genes exhibit significant differences in expression in tumor spheres formed from cervical cancer cell lines in reduced concentrations of L-glutamine (0.5% L-glutamine), as well as in glutamine starvation (0% L-glutamine).

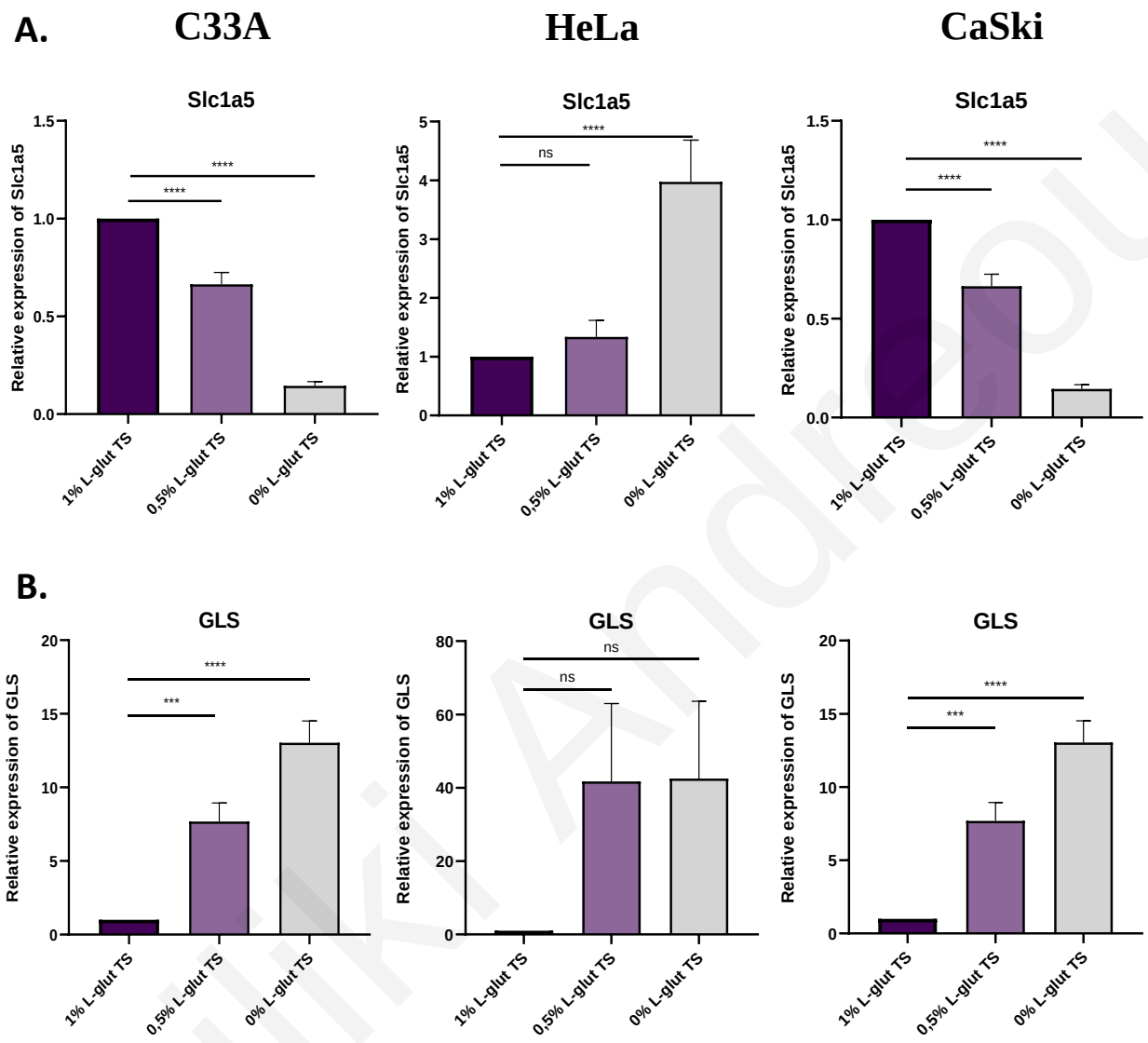


**Figure 11. Glutamine transporter, *Slc1a5*, and glutaminase enzyme, *GLS*, expression is deregulated in tumor spheres derived from Cervical cancer cells in reduced concentrations of L-glutamine.** Relative expression of **(A)** *Slc1a5* and **(B)** *GLS* in tumor spheres formed from cervical cancer cells, C33A, HeLa and CaSki, in different concentrations of L-glutamine (1%, 0.5% and 0%), was analyzed by RT-qPCR. *Actin* expression was used for normalization. Data presented as mean ± SEM of three biological replicates and are representative of three independent experiments. Statistical significance was evaluated using the one-way ANOVA statistical test. P <0.05 was considered statistically significant. (ns = non-significant, *p<0.05, **p<0.01, ***p<0.001, ****p<0.0001).

### 3.4 Glutamine metabolism-related genes are deregulated in HPV (+) compared to HPV (-) cervical cancer cells

Since we have identified differences in the expression of glutamine metabolism-related genes in tumor spheres formed from cervical cancer cells in different concentrations of L-glutamine, we further wanted to interrogate whether there are differences in the expression of glutamine transporters and enzymes in the adherent cervical cancer cells, that are either HPV (-) (C33A) or HPV (+) (HeLa and CaSki). In order to do that, we performed RT-qPCR analysis using the cervical cancer cells C33A, HeLa and CaSki to check the expression of 4 different glutamine transporters, *Slc1a5*, *Slc7a5*, *Slc38a3* and *Slc7a8* (**Figure 12A**) and 4 different glutamine metabolism-related enzymes, *GLS*, *GLS2*, *GSS*, and *Glud1* (**Figure 12B**). This analysis revealed that *Slc1a5* and *Slc7a8* were significantly downregulated, while *Slc7a5* was significantly upregulated in the HPV (+) HeLa and CaSki cells, compared to the HPV (-) C33A cells. However, *Slc38a3* expression was not significantly changed in HeLa and CaSki, compared to C33A cervical cancer cells (**Figure 12A**). Regarding the different glutamine metabolism-related enzymes tested, our analysis showed that the relative expression of *GLS* and *GLS2* was only significantly increased in HeLa cells, while *GLS2* expression was also increased in the HPV (+) CaSki cells, compared to the HPV (-) C33A. Moreover, *GSS* and *Glud1* expression was significantly decreased in HeLa cells, compared to C33A cells (**Figure 12B**). Overall, our results suggest that these glutamine metabolism-related transporters and enzymes are variably in cervical cancer cell lines, not always in a consistent manner to HPV status.

### 3.5 Generation of C33A cells, expressing the HPV16 oncogenes, E6, E7 and E6E7

To elucidate whether the changes in expression of the different glutamine metabolism-related genes between the HPV (-) and HPV (+) cervical cancer cell lines, are partially due to the presence of the E6/E7 viral oncogenes, and not purely a result of differences in genetic background of the cells, we have used C33A cells, that do not express the oncogenes, and transduced them using retroviral constructs that express the HPV16 oncogenes, E6 and E7, either alone (C33A E6, C33A E7) or together (C33A E6E7) (**Figure 13A**).

## A. Glutamine transporters

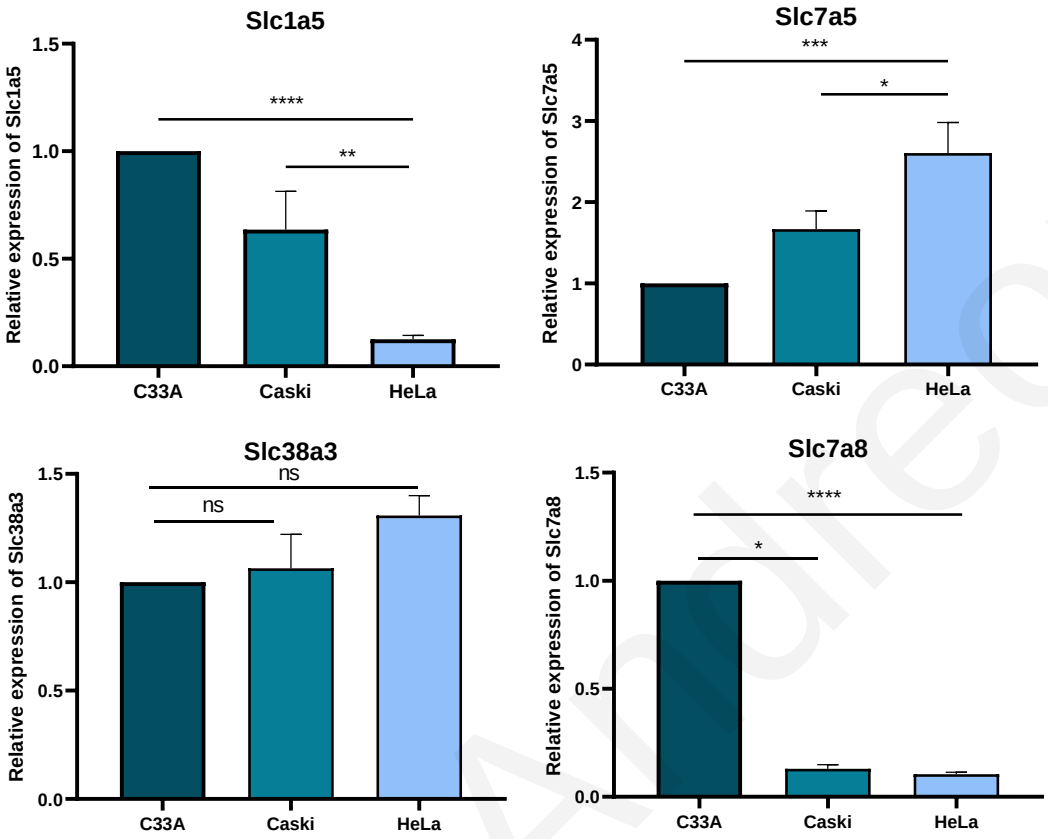


## B. Glutamine-related enzymes

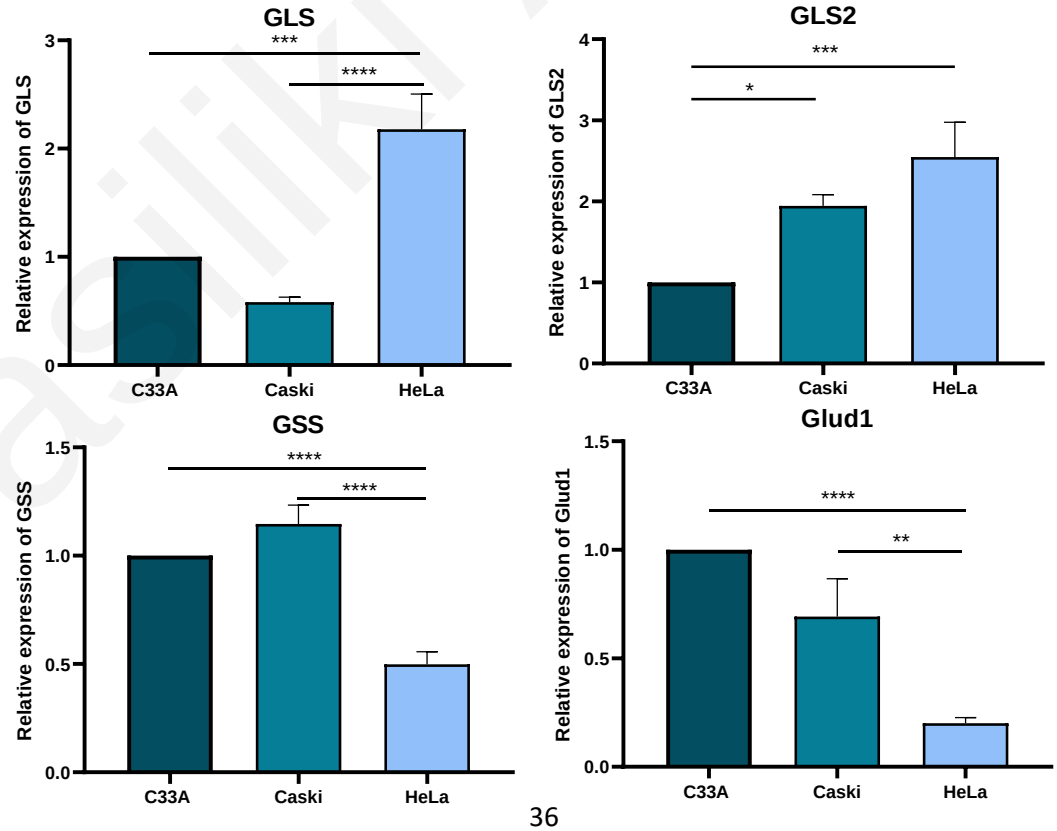

**Figure 12. Glutamine metabolism-related genes are deregulated in HPV (+) compared to HPV (-) cervical cancer cells.** Relative expression of **(A)** glutamine transporters (*Slc1a5, Slc7a5, Slc38a3, Slc7a8*) and **(B)** enzymes (*GLS, GLS2, GSS, Glud1*) in HPV (-) C33A and HPV (+) CaSki and HeLa cervical cancer cells, was analyzed by RT-qPCR. *Actin* expression was used for normalization. Data presented as mean ± SEM of three biological replicates and are representative of three independent experiments. Statistical significance was evaluated using the one-way ANOVA statistical test. P <0.05 was considered statistically significant. (ns = non-significant, *p<0.05, **p<0.01, ***p<0.001, ****p<0.0001).

Importantly, after the transduction and selection of the C33A cells that express the retroviruses of interest (pLXSN-empty, pLXSN-E6, pLXSN-E7, pLXSN-E6E7), we verified this expression by performing PCR, using E6- and E7-specific primers (**Figure 13B**).

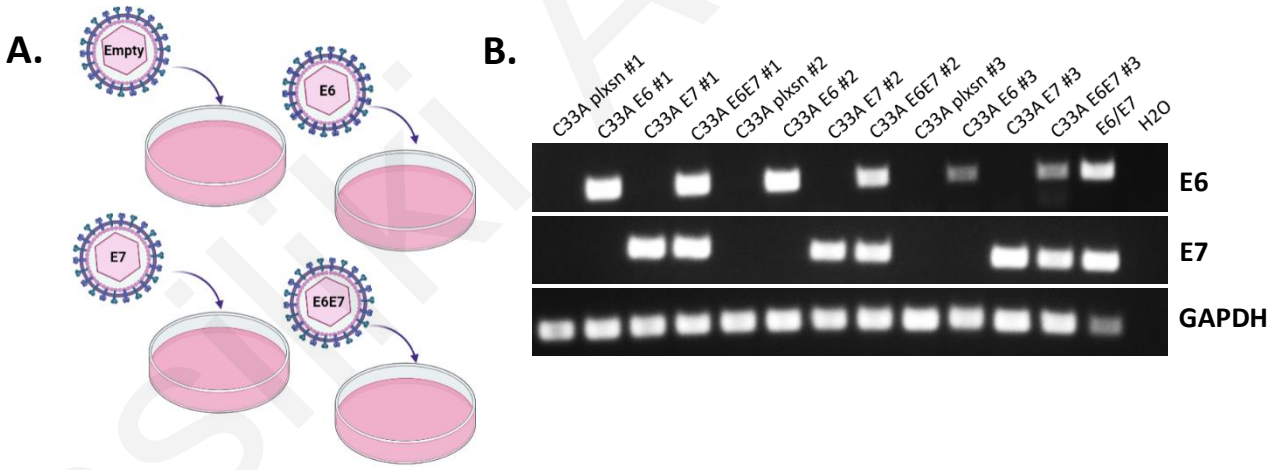


**Figure 13. Generation of C33A cells, expressing the HPV16 oncogenes, E6, E7 and E6E7.** HPV (-) cervical cancer cells C33A were transduced with the pLXSN-empty, pLXSN-HPV16E6, pLXSN-HPV16E7 and pLXSN-HPV16E6E7 vectors. **(A)** Schematic representation of the transduction of C33A cells with the retroviral vectors expressing the viral oncogenes. The figure was created with the use of BioRender.com web application. **(B)** Successful transduction of C33A cells with HPV16 viral oncogenes is illustrated by PCR using *E6*- and *E7*-specific primers. *GAPDH* was used as the loading control.

### 3.6 Glutamine metabolism-related genes are upregulated in the presence of HPV16 E7 and E6E7

To interrogate whether the viral oncogenes are responsible for the differences in expression of glutamine metabolism-related genes in cervical cancers, we performed RT-qPCR analysis for the 4 different glutamine transporters (*Slc1a5*, *Slc7a5*, *Slc38a3*, *Slc7a8*) and 4 glutamine metabolism-related enzymes (*GLS*, *GLS2*, *GSS*, *Glud1*), using the transduced C33A cells expressing the HPV16 oncogenes E6, E7 and E6E7. Interestingly, we have found that the presence of HPV16 E7 and HPV16 E6E7 resulted in significantly increased expression of all glutamine transporters tested, compared to the pLXSN control. Notably, *Slc7a5* was also upregulated in the presence of HPV16 E6 (**Figure 14A**). Furthermore, regarding the glutamine metabolism-related enzymes, our analysis revealed that expression of HPV16 E7 and HPV16 E6E7, resulted in significantly enhanced expression of *GLS* and *Glud1*, compared to the control. *GLS2* was also upregulated in the presence of HPV16 E6, while *GSS* demonstrated increased expression only in the presence HPV16 E6E7 (**Figure 14B**). Taken together, our results suggest that E7-expressing C33A cervical cancer cells exhibit increased expression of key glutamine transporters and enzymes, compared to C33A cells not expressing the HPV16 E7 oncogene.

### 3.7 The HPV16 E6 and E7 oncogenes increase extracellular glutamine and decrease extracellular glutamate levels

To explore whether the functionality of glutamine metabolism is affected in the presence and absence of the HPV16 oncogenes E6 and E7, we checked the levels of the metabolites glutamine and glutamate in the cell culture medium. Cells were starved of glutamine for two and a half hours, followed by replenishment of medium containing 2mM of L-glutamine to allow consumption by the cells for 30 minutes. After half an hour, the cell culture medium was harvested, and the consumption assay was performed.

## A. Glutamine transporters

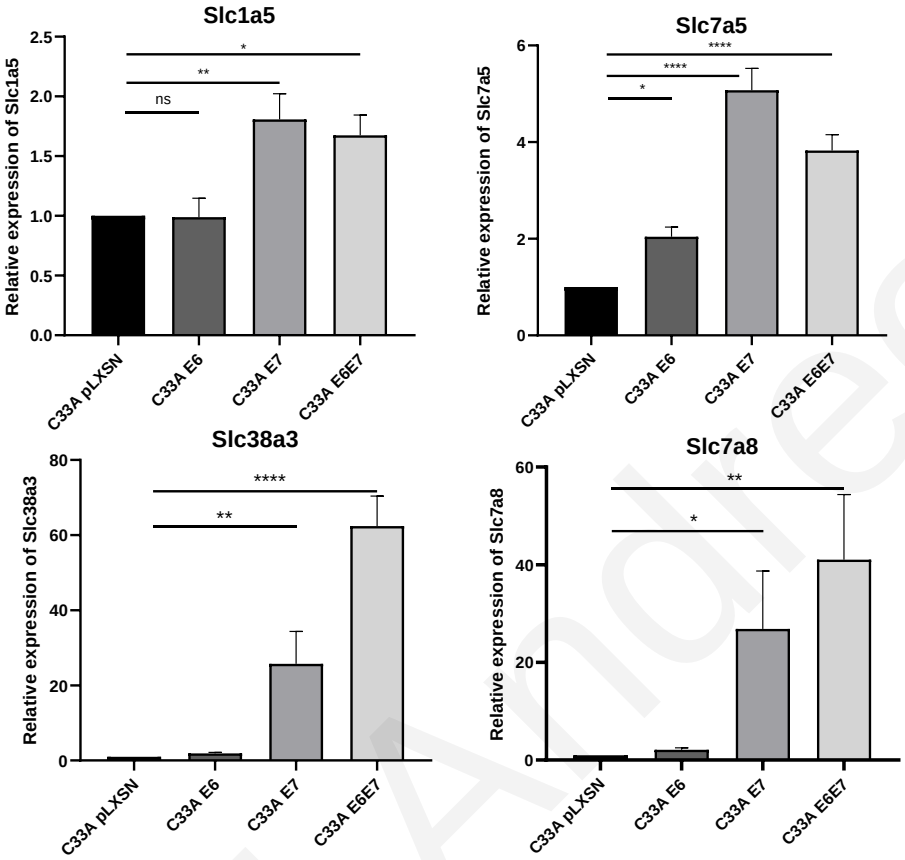


## B. Glutamine-related enzymes

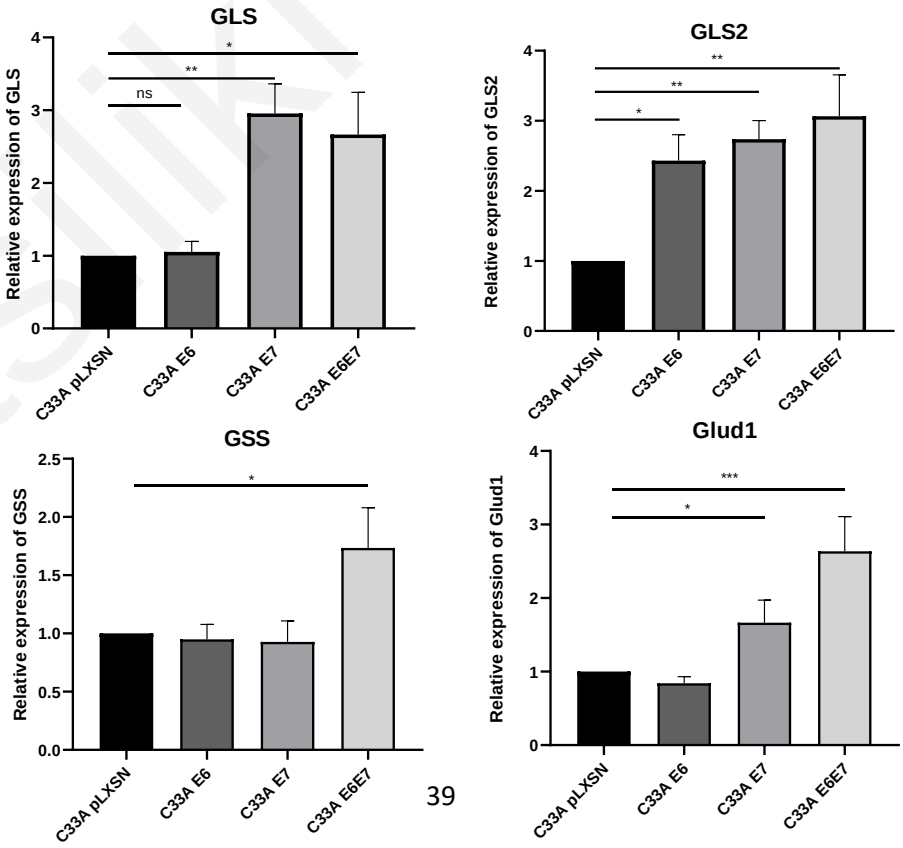

**Figure 14. Glutamine metabolism-related genes are upregulated in the presence of HPV16 E7/E6E7.** Relative expression of **(A)** glutamine transporters (*Slc1a5, Slc7a5, Slc38a3, Slc7a8*) and **(B)** glutamine-related enzymes (*GLS, GLS2, GSS, Glud1*) in tumor spheres formed from the C33A cells expressing E6, E7 and E6E7, was analyzed by RT-qPCR. *Actin* expression was used for normalization. Data presented as mean ± SEM of three biological replicates and are representative of three independent experiments. Statistical significance was evaluated using the one-way ANOVA statistical test. P <0.05 was considered statistically significant. (ns = non-significant, *p<0.05, **p<0.01, ***p<0.001, ****p<0.0001).

During the glutamine-glutamate consumption assay, glutamine is converted into glutamate by the addition of the glutaminase enzyme. Oxidation of glutamate is catalyzed by the glutamate dehydrogenase enzyme, along with the reduction of $NAD^+$ to NADH. In the presence of NADH, reductase reduces its substrate, pro-luciferin to luciferin, which is detected in a luciferase reaction. The amount of light produced is proportional to the amount of glutamate in the sample (**Figure 15A**).

Using the glutamine-glutamate consumption assay, we measured the extracellular glutamine and glutamate levels in transduced-C33A cells expressing E6, E7 or E6E7, to assess whether there are any differences. Glutamine levels in the cell culture medium were significantly increased in cells expressing E7 and E6E7, compared to the pLXSN control. An increase was also observed for the E6-expressing C33A cells, compared to the control, nevertheless the difference was not statistically significant (**Figure 15B**). Interestingly, the opposite trend was revealed for extracellular glutamate levels. Glutamate concentration in the cell culture medium, which was calculated based on the glutamate titration curve (**Figure 15C**), decreased around 2μM in E6-, E7- and E6E7-expressing cells, compared to the control (**Figure 15D**). These results demonstrate that the viral oncoproteins E6 and E7 alter the levels of the metabolites glutamine and glutamate.

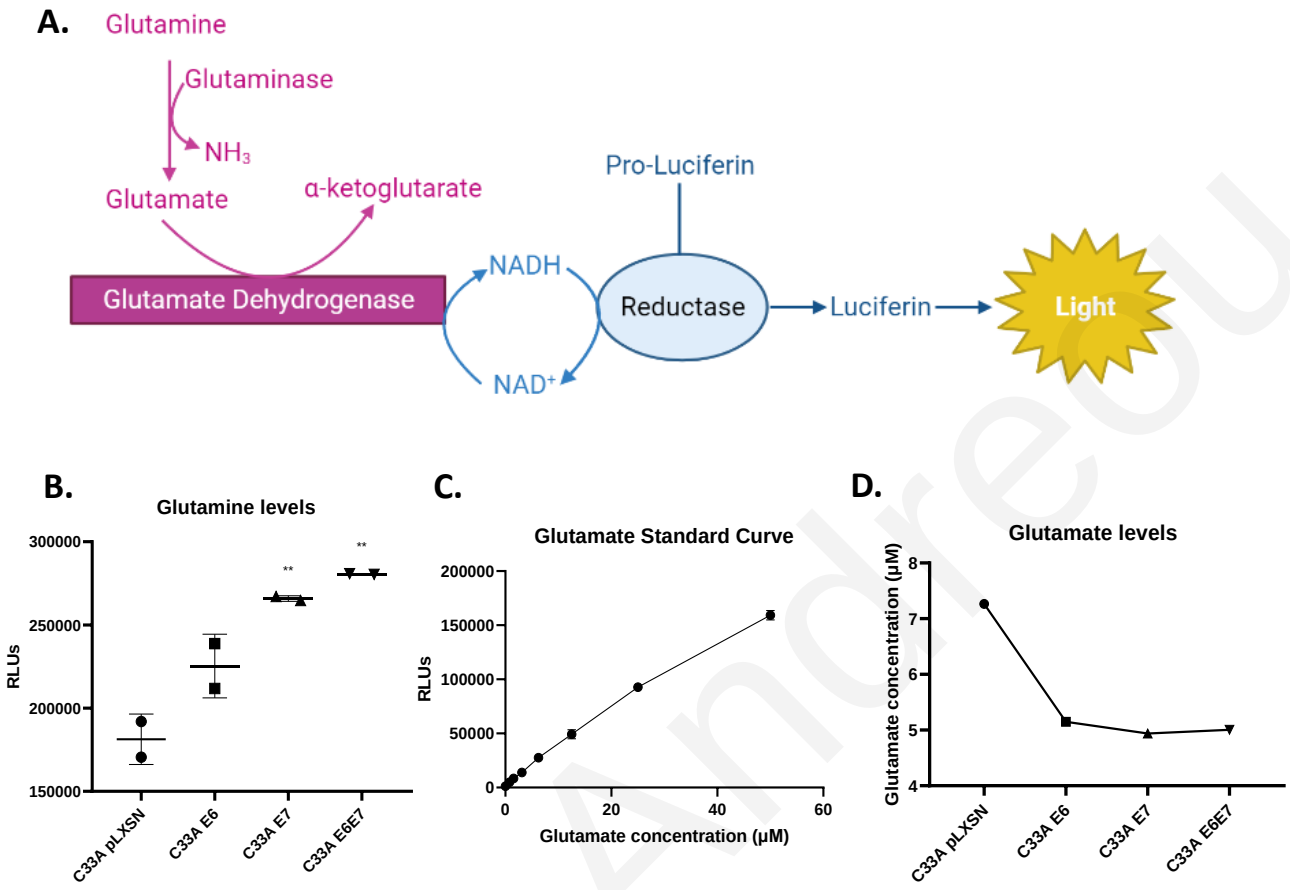


**Figure 15. The HPV16 E6 and E7 oncogenes increase extracellular glutamine and decrease extracellular glutamate levels. (A)** Schematic diagram of the Glutamine/glutamate assay principle, based on manufacturer's instructions (Promega). The figure was created with the use of BioRender.com web application. **(B)** Glutamine levels are monitored in transduced C33A cells expressing the HPV16 oncogenes E6, E7 or E6E7. Glutamine levels are proportional to RLUs (Relative Light Units). Each dot represents a technical replicate. **(C)** Glutamate titration curve, created using two-fold serial dilutions of glutamate controls prepared in PBS, starting from 50µM. **(D)** Glutamate levels are monitored in transduced C33A cells expressing the HPV16 oncogenes E6, E7 or E6E7. Glutamate concentration for each condition was calculated based on the glutamate titration curve, using the GraphPad Prism software (8.0.1). Data presented as mean ± SEM of two biological replicates and are representative of a single experiment. Statistical significance was evaluated using the one-way ANOVA statistical test. P <0.05 was considered statistically significant. (ns = non-significant, *p<0.05, **p<0.01, ***p<0.001, ****p<0.0001).

### 3.8 HPV16 E7-expressing cervical cancer cells become less sensitive to glutamine starvation

Since we have found that the presence of the HPV16 E7 oncogene, promotes the transcriptional upregulation of several important genes involved in glutamine metabolism, we consequently questioned whether the E7 expression could possibly influence the sphere-forming capabilities of the C33A cervical cancer cells, in different concentrations of L-glutamine. To further investigate this, we performed the *in vitro* tumor sphere formation assay, using the transduced-C33A cells (C33A-pLXSN, C33A E6, C33A E7, C33A E6E7) in medium containing 1%, 0.5% or 0% L-glutamine. On day 5, day 7 (**Appendix 2**) and day 10 (**Figure 15**) of the assay, representative images were taken for all different cell lines and conditions tested. As shown in **Figure 16**, tumor spheres formed in 0.5% L-glutamine concentration, did not exhibit significant differences in number or size, compared to the control. Remarkably, we detected that C33A cells expressing the HPV16 E7 oncogene formed tumor spheres that were increased in number and larger in size, in the 0% L-glutamine concentration, in comparison to the C33A pLXSN. Similar phenotype was also observed for the tumor spheres that derived from the HPV16 E6E7-expressing cells, in glutamine starvation (0% L-glutamine) (**Figure 15**). Our results come in agreement and alignment with the data of our transcriptional analysis and suggest that cervical cancer cells expressing the E7 oncogene, are less sensitive to the effects of glutamine starvation and efficiently maintain their clonogenic potential, even in the absence of this critical amino acid.

### 3.9 Stemness-related genes are enriched in tumor spheres formed from HPV-negative cervical cancer cells expressing the HPV16 oncogenes in glutamine starvation

To assess whether the tumor spheres formed from transduced-C33A cells, are enriched in the expression of stemness-related genes, we performed RT-qPCR analysis. For this analysis, C33A pLXSN adherent cells were used as the control for all the different cell lines. RT-qPCR analysis revealed that **s**temness genes tested (*Oct4, Sox2, Klf4, Nanog*), were significantly upregulated

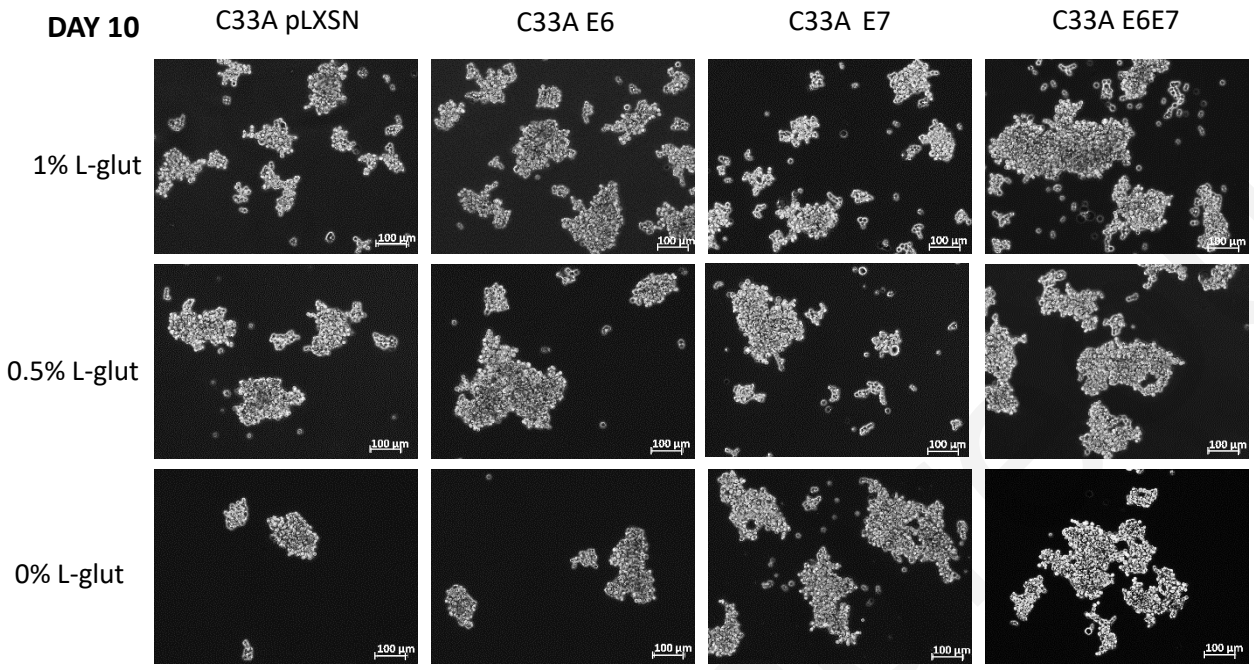


**Figure 16. E7-expressing cervical cancer cells become less sensitive to glutamine starvation effects.** Representative phase-contrast images of the tumor spheres formed from HPV-negative cervical cancer cells C33A, expressing the viral oncogenes (HPV16 E6, E7 or E6E7), in different concentrations of L-glutamine (1%, 0.5% and 0% L-glutamine). The images were taken on day 10 of the tumor spheres assay, using the 10x lens of the Axio camera (Zeiss Axio Observer.A1) and are representative of three independent experiments. Scale bars, 100μm.

only in C33A pLXSN tumor spheres formed in the 0% L-glutamine concentration, compared to the adherent cells (**Figure 17A**). Similarly, the expression of all stemness markers was increased in C33A E6 tumor spheres, in the 0% L-glutamine concentration, compared to the adherent pLXSN cells (**Figure 17B**). Furthermore, for C33A E7 tumor spheres, *Oct4* was significantly downregulated in 1% L-glutamine tumor spheres, compared to the pLXSN adherent cells. *Sox2* was significantly downregulated in all tumor spheres (1%, 0.5% and 0% L-glutamine tumor spheres), compared to the control. Importantly, the expression of *Sox2* was decreased in C33A E7 adherent cells, compared to the C33A pLXSN adherent. *Klf4* was significantly upregulated only in C33A E7 tumor spheres formed in the 0% L-glutamine concentration, compared to the

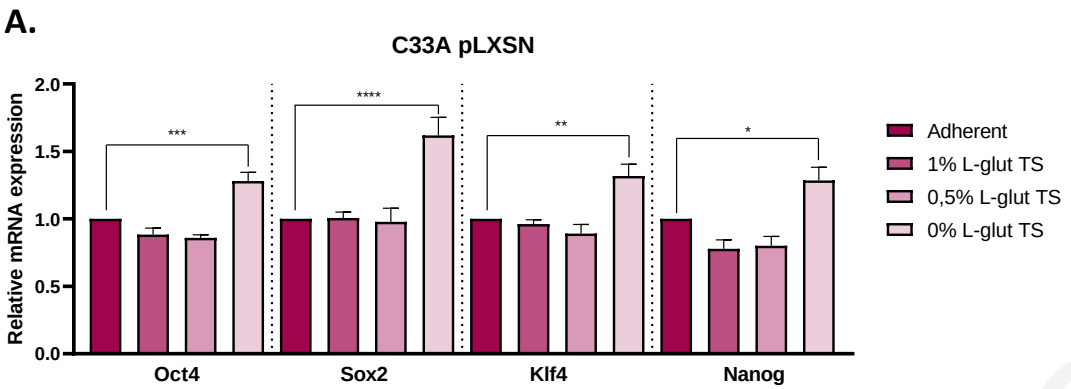


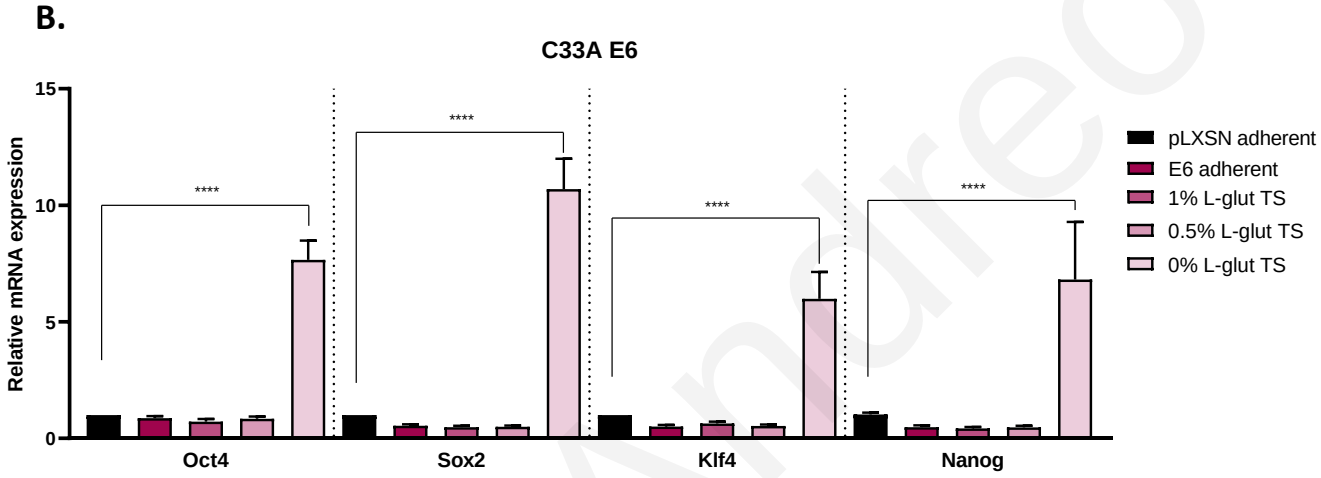


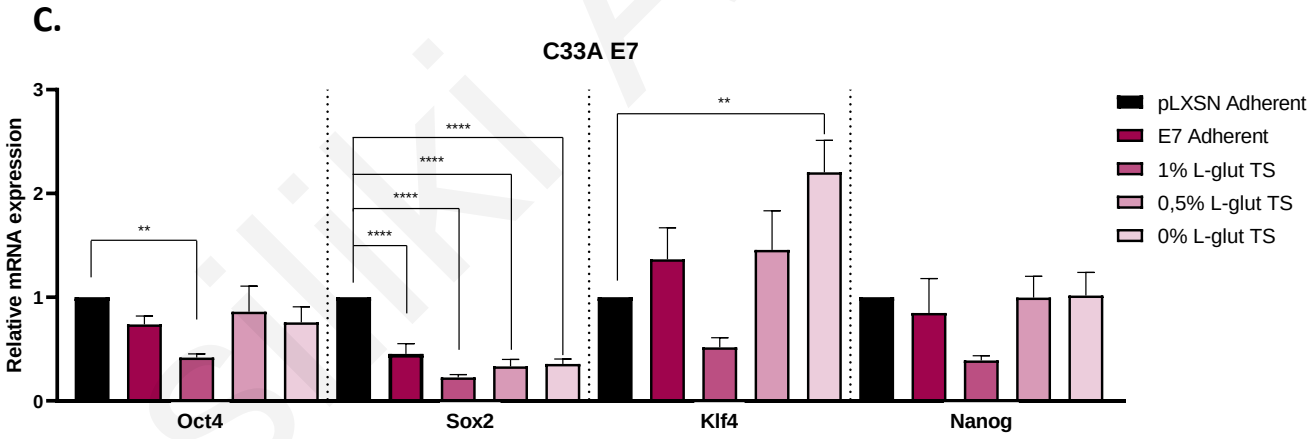


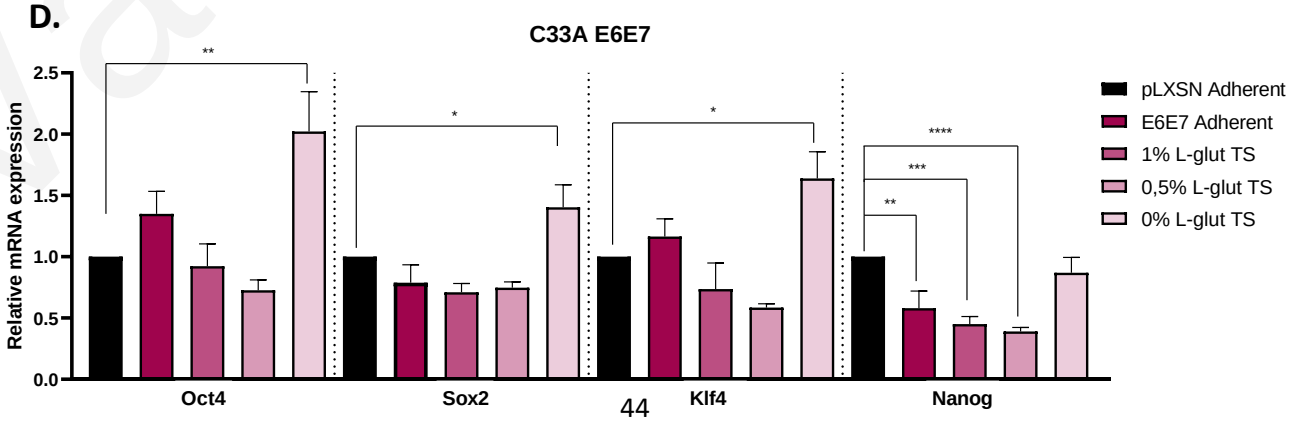

**Figure 17. Stemness-related genes are enriched in tumor spheres formed from HPV-negative cervical cancer cells expressing the HPV16 oncogenes in the glutamine starvation.** RT-qPCR was performed to examine the expression of stemness genes *Oct4, Sox2, Klf4, and Nanog,* in the tumor spheres population formed from C33A cells expressing the HPV16 oncogenes (E6/E7/E6E7) in different concentrations of L-glutamine (1%, 0.5%, 0% L-glutamine) compared to the C33A pLXSN adherent cells, **(A)** C33A pLXSN, **(B)** C33A E6, **(C)** C33A E7 and **(D)** C33A E6E7. *Actin* expression was used for normalization. Data presented as mean ± SEM of three biological replicates and are representative of three independent experiments. Statistical significance was evaluated using the one-way ANOVA statistical test. P <0.05 was considered statistically significant. (ns = non-significant, *p<0.05, **p<0.01, ***p<0.001, ****p<0.0001).

adherent cells, while *Nanog* expression did not exhibit any significant changes between adherent cells and tumor spheres (**Figure 17C**). In C33A E6E7 tumor spheres, *Oct4*, *Sox2* and *Klf4* expression was significantly increased in tumor spheres formed in glutamine starvation (0% L-glutamine), compared to the C33A pLXSN adherent cells. Additionally, *Nanog* demonstrated significantly decreased expression in tumor spheres formed in 1% and 0.5% L-glutamine concentrations, compared to the pLXSN adherent cells. Notably, *Nanog* expression was significantly decreased also in C33A E6E7 adherent, compared to the C33A pLXSN adherent cells (**Figure 17D**).

### 3.10 Glutamine starvation reduces the number of tumor spheres formed

Our tumor sphere assay performed using the transduced-C33A cells, revealed that the presence of the HPV16 E7 oncogene, resulted in the formation of more tumor spheres in the 0% L-glutamine concentration, compared to the pLXSN control, as shown in representative images (**Figure 16**). Nevertheless, we further needed to quantify the differences observed, and in order to do that, we manually counted the tumor spheres formed at day 10 of the assay, in a specific area that was defined in each well of the 6-well plate (**Figure 8**), for all the different cell lines

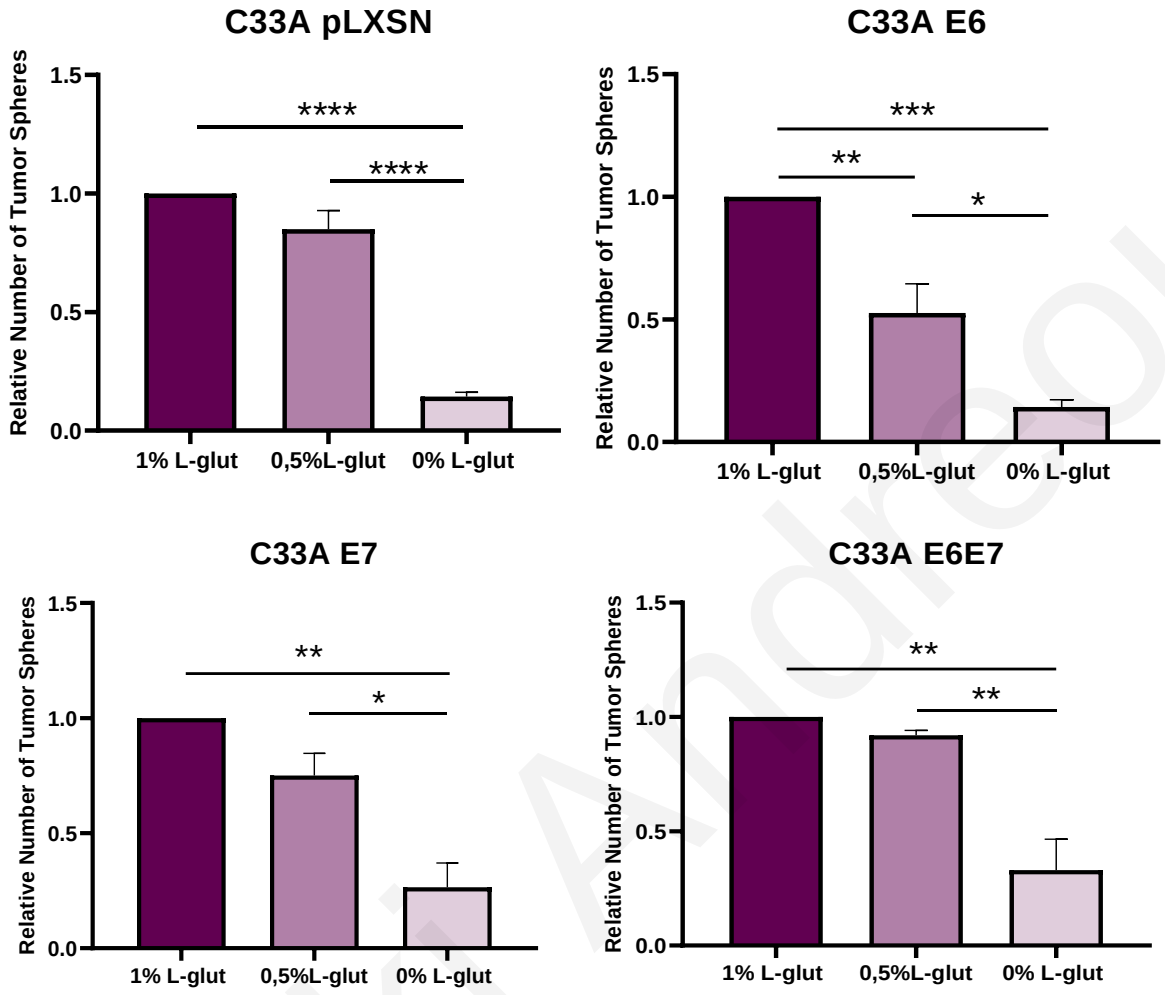


**Figure 18. Glutamine starvation reduces the number of tumor spheres formed.** Relative numbers of tumor spheres formed using the different cell lines C33A pLXSN, C33A E6, C33A E7 and C33A E6E7, in different concentrations of L-glutamine (1%, 0.5% and 0% L-glutamine) were plotted, using the GraphPad Prism software 8.0.1. Data presented as mean ± SEM of three biological replicates and are representative of three independent experiments. Statistical significance was evaluated using the one-way ANOVA statistical test. P <0.05 was considered statistically significant. (ns = non-significant, *p<0.05, **p<0.01, ***p<0.001, ****p<0.0001).

(C33A-pLXSN, C33A E6, C33A E7, C33A E6E7) and conditions tested (1%, 0.5% and 0% L-glutamine). Our quantification analysis exhibited that the absolute (**Appendix 3**) as well as the relative number of tumor spheres formed in the 0% L-glutamine concentration was significantly

decreased, compared to the 1% L-glutamine control concentration, for all the different cell lines tested (**Figure 18**). These results are in line with our previous observations, showing that cervical cancer cells demonstrate an impaired ability to form tumor spheres in the setting of glutamine starvation.

### 3.11 E7-expressing cells form more tumor spheres, in all glutamine concentrations, including glutamine starvation, compared to the pLXSN

In addition to the differences in number of tumor spheres formed between the different concentrations of L-glutamine, within the same cell line, we further wanted to gain insights into the differences in number of tumors spheres formed between the different cell lines, within the same L-glutamine concentration, therefore we used the quantification data and performed this different comparison. Interestingly, this analysis revealed that the number of tumor spheres derived from the C33A E7-expressing cells was significantly increased, compared to the C33A pLXSN control, in all different L-glutamine concentrations (1%, 0.5% and 0% L-glutamine). Notably, in glutamine starvation (0% L-glutamine concentration), more tumor spheres were formed in E7- and E6E7-expressing C33A cells, compared to the pLXSN control (**Figure 19**). This result further reinforces our observations, showing that the expression of HPV16 E7 promotes the formation tumor spheres, even in the complete devoid of L-glutamine.

### 3.12 Oncogene-expressing cervical cancer cells form larger tumor spheres in glutamine starvation

Besides the differences in the number of tumor spheres formed from the HPV16 E7-expressing C33A cervical cancer cells, we further wanted to interrogate whether there are any differences in the size of tumor spheres formed as well. In order to do that, we manually counted 20 tumor spheres formed on day 10 of the assay, in the specific area that was defined in each well of the 6-well plate (**Figure 8**), and measured the diameter of each tumor sphere, for all the

different cell lines (C33A-pLXSN, C33A E6, C33A E7, C33A E6E7) and conditions tested (1%, 0.5% and 0% L-glutamine). After measuring the diameter length, using the Axio Vision software

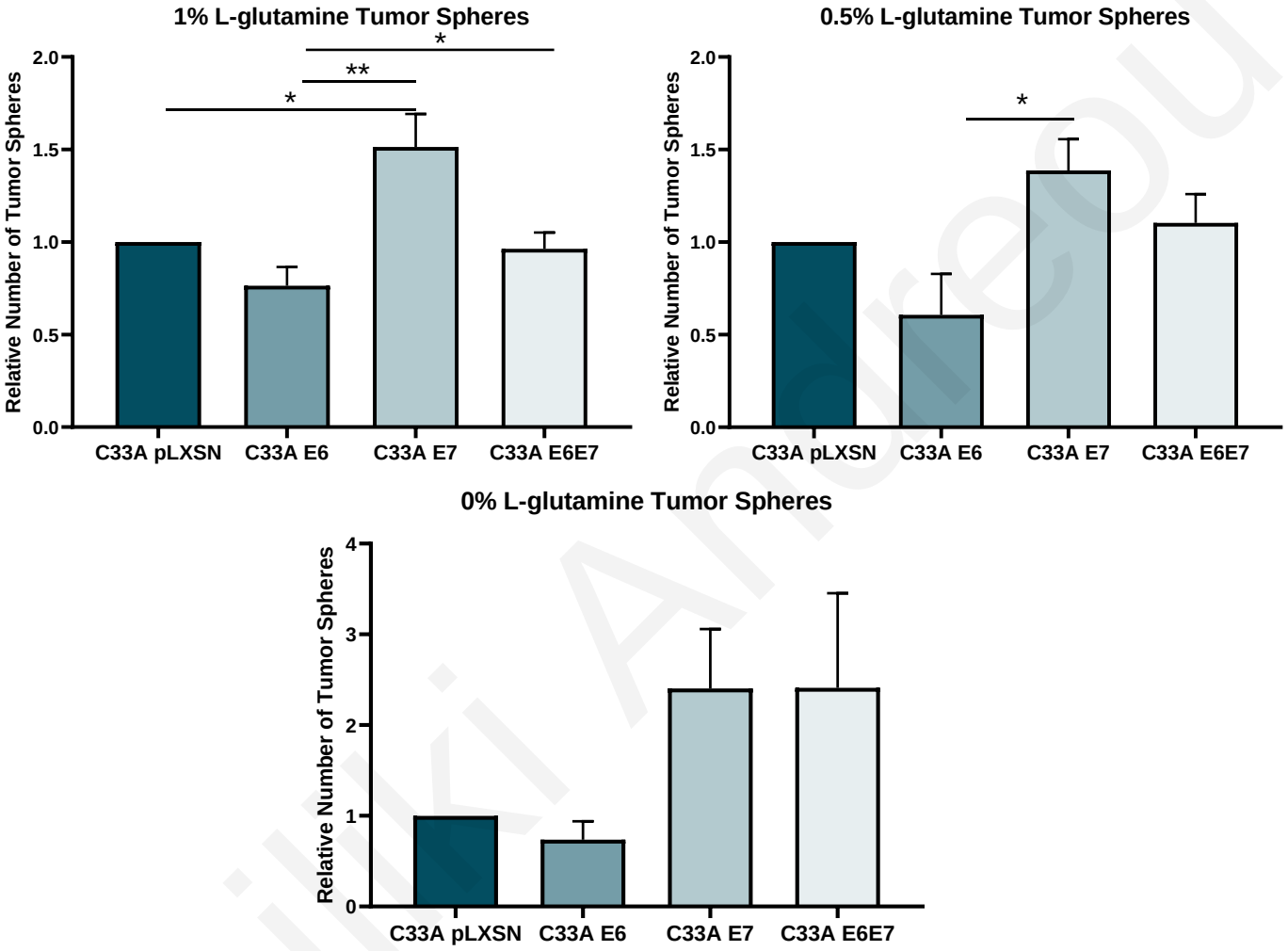


**Figure 19. E7-expressing cells form more tumor spheres, in all L-glutamine concentrations, including glutamine starvation, compared to the pLXSN.** Relative numbers of tumor spheres formed using the different cell lines C33A pLXSN, C33A E6, C33A E7 and C33A E6E7, in different concentrations of L-glutamine (1%, 0.5% and 0% L-glutamine) were plotted, using the GraphPad Prism software 8.0.1. Data presented as mean ± SEM of three biological replicates and are representative of three independent experiments. Statistical significance was evaluated using the one-way ANOVA statistical test. P <0.05 was considered statistically significant. (ns = non-significant, *p<0.05, **p<0.01, ***p<0.001, ****p<0.0001).

we categorized the tumor spheres based on their diameter size, in 3 different categories, >300μm, 200-300μm and 100-200μm. We found that C33A pLXSN cells formed less tumor spheres of large size (>300μm, 200-300μm) in the 0% L-glutamine concentration, while for all the other cell lines, C33A E6, C33A E7 and C33A E6E7, more tumor spheres of larger size are formed in glutamine starvation (**Figure 20**). These results corroborate that the phenotype associated with increased size of tumor spheres is linked specifically to the presence of the HPV16 oncogenes.

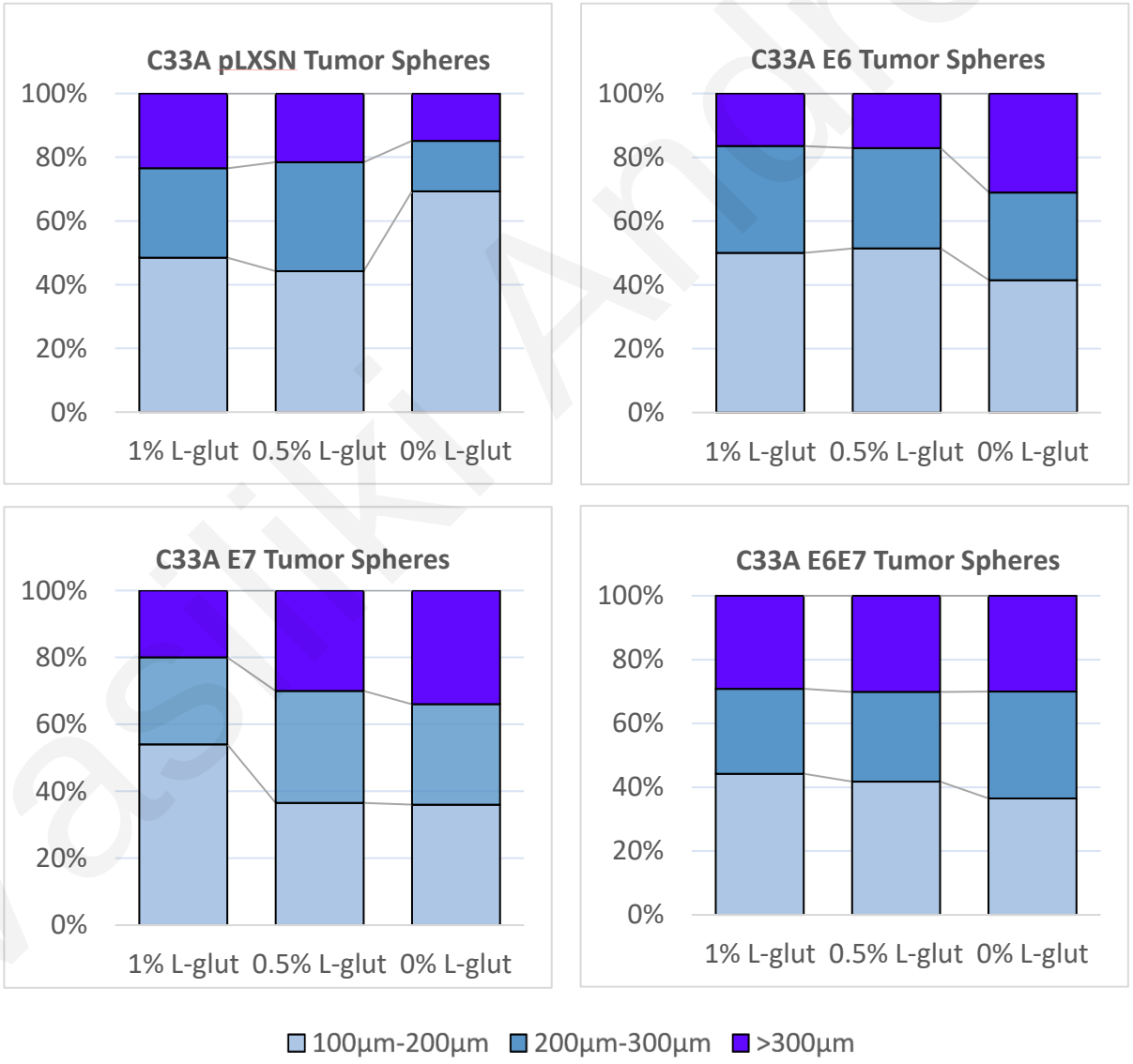

**Figure 20. Oncogene-expressing cervical cancer cells form larger tumor spheres in glutamine starvation.** 20 tumor spheres of each condition C33A pLXSN, C33A E6, C33A E7 and C33A E6E7, in different concentrations of L-glutamine (1%, 0.5% and 0% L-glutamine), were counted and categorized based on their diameter length (100μm-200μm, 200μm-300μm and >300μm). Data presented as mean of three biological replicates and are representative of three independent experiments. The data of this analysis were plotted using Microsoft PowerPoint.

### 3.13 Oncogene-expressing cells are less sensitive glutamine starvation

Additionally, apart from revealing the differences in size of tumor spheres formed between the different concentrations of L-glutamine, within the same cell line, we further wanted to gain an insight into the differences in size of tumors spheres formed between the different cell lines, within the same L-glutamine concentration, therefore we used the diameter length data and performed this different comparison. Differences were observed for the 1% L-glutamine. Of note, however, in the 0.5% L-glutamine concentration, more tumor spheres of larger size (>300μm, 200-300μm) were formed in the presence of HPV16 E7, while in glutamine starvation more tumor spheres of larger size were formed from HPV16 E6, HPV16 E7 and HPV16 E6E7-expressing cells (**Figure 21**).

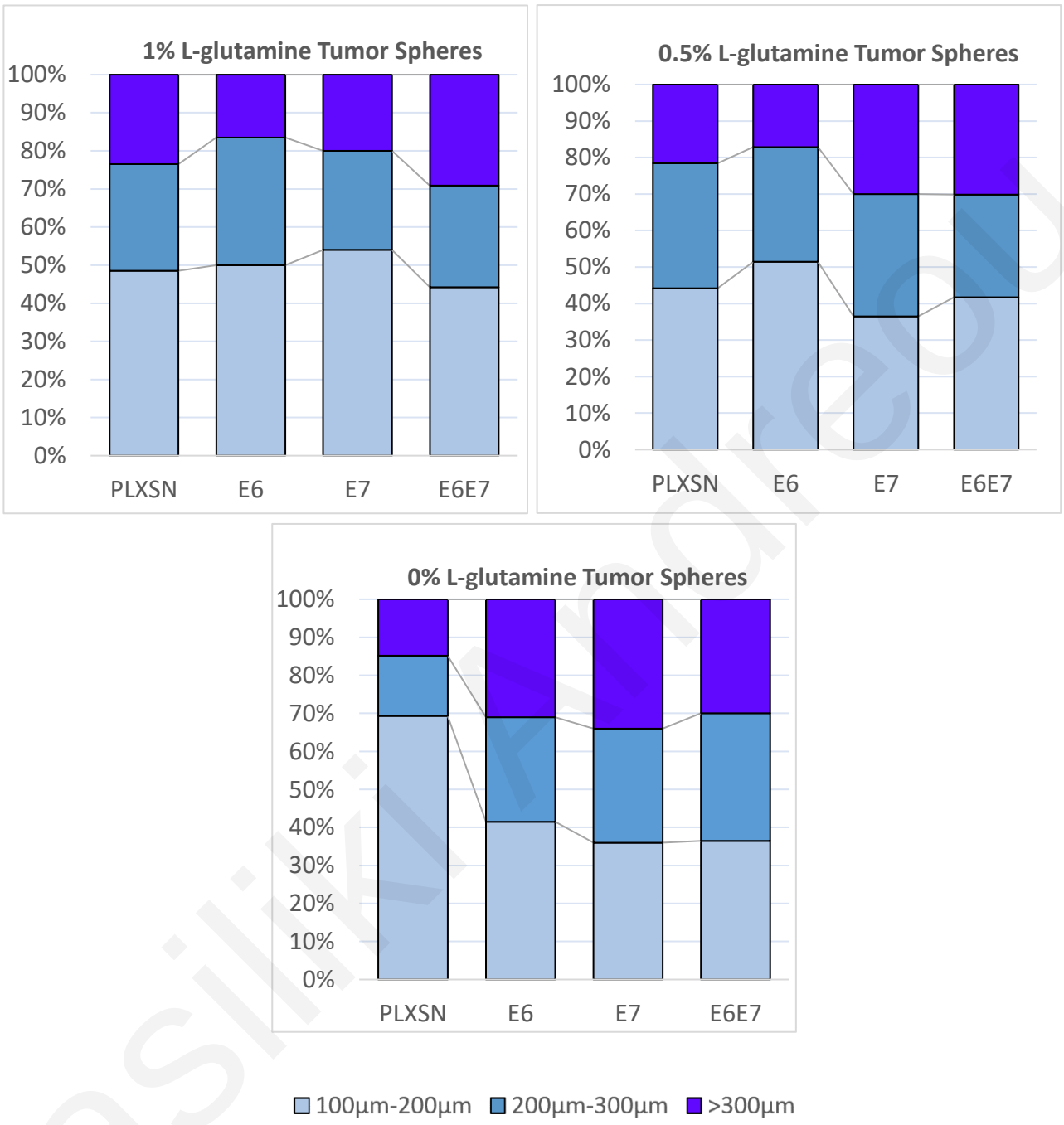


**Figure 21. Oncogene-expressing cells are less sensitive in glutamine starvation.** 20 tumor spheres of each cell line C33A pLXSN, C33A E6, C33A E7 and C33A E6E7, formed in different concentrations of L-glutamine (1%, 0.5% and 0% L-glutamine), were counted and categorized based on their diameter length (100μm-200μm, 200μm-300μm and >300μm). Data presented as means of three biological replicates and are representative of three independent experiments. The data were plotted using Microsoft PowerPoint.

# 4. DISCUSSION

During carcinogenesis, cancer cells promote metabolic reprogramming, an emerging hallmark of cancer (Hanahan, Douglas, Weinberg 2011, Ward, Thompson 2012), which remodels various metabolic pathways to fulfill the energy requirements and sustain rapid proliferation of malignant cells (Schiliro, Firestein 2021, Martínez-Reyes, Chandel 2021). Even though "Warburg effect" has been the most well-established feature of metabolic reprogramming, increasing evidence supports that cancer cells depend on glutamine metabolism for their survival, growth, and proliferation (Yang, L. et al. 2017). Nevertheless, the precise mechanisms that are used by cancer cells to rewire glutamine metabolism remain unclear.

Several lines of evidence revealed that glutaminolysis, the conversion of glutamine into glutamate, is increased in many cancer types, such as glioma (Ekici et al. 2020), breast (Demas et al. 2019), and ovarian cancer (Yuan et al. 2015). Additionally, glutamine metabolism-related transporters and enzymes have been shown to exhibit elevated expression in different types of cancer, promoting glutamine dependence (Bhutia, Ganapathy 2016, Matés et al. 2019). Importantly, further studies suggest that tumor cells induce the metabolic reprogramming of the glutamine pathway, at least in part, through the action of oncogenes and tumor suppressors, such as *c-Myc* (Wise et al. 2008) and *pRb* (Reynolds et al. 2014). These findings potentially convey that other oncogenes and tumor suppressors could possibly be involved and be accountable for remodeling glutamine metabolism in cancers.

Cervical cancer has been acknowledged to be the fourth most frequently diagnosed cancer among women globally (Arbyn et al. 2020, Bray et al. 2018), with HPV infection to be detected in around 90% of the total cases (Bouvard et al. 2009). The HPV16 oncogenes, E6 and E7 have been established to significantly contribute to carcinogenesis through several processes, including metabolic reprogramming (Mittal, Banks 2017). Nevertheless, it is intriguing that the viral oncogenes have not been adequately examined in promoting metabolic reprogramming by deregulating glutamine metabolism in cervical cancers.

The main aim of this study was to investigate whether the oncogenes of HPV16, E6 and E7, contribute to the remodeling of glutamine metabolism in cervical cancers. In an effort to address this, we used the *in vitro* tumor sphere formation assay to evaluate whether the clonogenic potential of HPV (+) (HeLa, CaSki) and HPV (-) (C33A) cervical cancer cells is affected when

glutamine metabolism is impaired or suppressed. Notably, an approach to suppress glutamine metabolism is to limit the availability of glutamine itself (Le 2021), thereby the tumor sphere formation assay was performed in reduced or complete absence of glutamine. We showed that in the setting of glutamine starvation (0% L-glutamine), the sphere-forming capacity of cervical cancer cells was significantly decreased compared to the normal glutamine concentration (1% L-glutamine), since less and smaller in size tumor spheres were formed, regardless of HPV presence. This suggests that cervical cancer cells demonstrate an impaired ability to form tumor spheres in the absence of glutamine. In addition, we observed that in reduced glutamine supply (0.5% L-glutamine), there were no significant differences in the size or number of tumor spheres, compared to the control (1% L-glutamine), revealing that even in limited glutamine availability, the clonogenic potential of cervical cancer cells is not affected (**Figure 9**). Importantly, these findings concur with previous studies in the literature since it has been well-established that glutamine is a crucial amino acid for cancer cells and its absence results in decreased cell proliferation and cell death (Yuneva et al. 2007, Chiodi et al. 2019).

Tumor spheres have been established to be a useful three-dimensional *in vitro* model, which is frequently used in cancer research, since they are believed to provide a more relevant pathophysiological microenvironment of study. Notably, these tumor-derived spheroids are purposed for the enrichment of cells with Cancer Stem Cells (CSCs) activity or cells with stem-related characteristics (Tirino et al. 2013). To check whether the tumor spheres formed using HPV (+) and HPV (-) cervical cancer cells demonstrate increased expression of stemness markers, RT-qPCR analysis was performed. We showed that, indeed, cervical tumor spheres that are formed in different glutamine concentrations (1%, 0.5%, 0% L-glutamine) are enriched in stemness markers, including *Oct4*, *Sox2*, *Klf4* and *Nanog*. Remarkably, our analysis revealed that in tumor spheres that are formed in glutamine starvation, the expression of stemness markers was even higher (**Figure 10**). Importantly, these results are in agreement with the findings of previous studies, suggesting that glutamine starvation induces stemness properties in cancer cells, accompanied with increased expression of stemness markers (Prasad et al. 2021).

Furthermore, the transcriptional analysis we have performed revealed that glutamine transporters and glutamine metabolism-related enzymes demonstrated differential gene expression between HPV (+) and HPV (-) cervical cancer cells, however we did not identify any consistent expression pattern (**Figure 12**). Nevertheless, we questioned whether the presence of

the viral oncogenes, E6 and E7, was responsible for the differences observed. Considering that the different cervical cancer cell lines used for our transcriptional analysis have different genetic backgrounds that could potentially affect the outcome, we developed a different cellular system, where we transduced the HPV (-) C33A cells, to express E6 and E7, either alone or together (**Figure 13**).

Subsequently, our transcriptional analysis performed using the E6-, E7- and E6E7-expressing C33A cells demonstrated that glutamine transporters, including *Slc1a5*, *Slc7a5, Slc7a5, Slc38a3*, as well as glutamine metabolism-related enzymes, such as *GLS*, *GLS2* and *Glud1*, exhibited elevated expression in E7- and E6E7-expresssing cells (**Figure 14**). These findings suggest that the presence of the E7 oncogene upregulates key players of glutamine metabolism, potentially enhancing glutamine consumption and promoting glutaminolysis in HPV-related cervical cancers. Importantly, our results are consistent with the findings of previous studies, showing that glutamine transporters and enzymes are overexpressed in different cancer types (Bhutia, Ganapathy 2016, Matés et al. 2019). In addition, our data are in line with a study published in January 2023, by Ortiz-Pedraza et al. in *Viruses*, where they also observed upregulation of glutamine metabolism-related genes in the presence of the HPV16 oncogenes (Ortiz-Pedraza et al. 2023).

Remarkably, the deregulation of key genes involved in the glutamine pathway is also evident in the results of the analysis we have conducted using data from the Cancer Genome Atlas (TCGA) CESC dataset and the GTEx database, comparing cervical tumors with normal tissues. The findings of this analysis are in line with the results of our transcriptional data, demonstrating that the main glutamine transporters, *Slc1a5* and *Slc7a5*, as well as the enzymes *GLS2* and *GSS* are significantly overexpressed in cervical tumors compared to normal tissues (**Figure 22**). These promising findings indicate that glutamine metabolism and its key components could serve as potential therapeutic targets for cervical cancers. This can be accomplished through pharmacological interventions with the implementation of dietary strategies, working together synergistically to maximize their therapeutic benefits (Taylor et al. 2022).

Additionally, to examine the involvement of E6 and E7 in the consumption of glutamine and glutamate in cervical cancer cells, we have performed a glutamine-glutamate consumption assay, which revealed that E7 and E6E7 significantly increased extracellular glutamine levels, while for the oncogene-expressing cells extracellular glutamate levels were decreased (**Figure 15**). These

findings seem to confirm that oncogenes modify glutamine and glutamate uptake of cancer cells (Ni et al. 2023, Kim, M. H., Kim 2013, Pavlova, Thompson 2016), potentially through increasing the expression of glutamine transporters and enzymes, such as glutaminase (Jin et al. 2016). However, our results differ from previous studies showing that extracellular glutamine levels decrease in cancer cells, since they increase its uptake to fulfill their high energy demands and continue to proliferate (Pavlova, Thompson 2016, Li, T., Le 2018). One possible explanation for our results could be that in cells that express E7, an increase in the expression of glutaminase can cause the release of glutamate, which can be taken up by neighboring cells and converted back to glutamine, by glutamine synthetase. As a result, extracellular glutamine can accumulate in the tumor microenvironment. As for glutamate, our findings are in agreement with some previous studies in the literature suggesting that extracellular glutamate levels can be reduced due to various reasons, including increased uptake by cancer cells or increased conversion of glutamate to other metabolites, which can be used for other metabolic pathways (Son et al. 2013, Timmerman et al. 2013). Overall, increased extracellular glutamine and decreased extracellular glutamate levels suggest a perturbation of glutamine-glutamate cycle in the presence of the viral oncogenes (Yoo et al. 2020). In any case, given that our findings are based only on a preliminary attempt and the experiment should be repeated, the results should be treated with the utmost caution, while we cannot proceed in drawing any safe conclusions.

We have revealed that the presence of E7 affects the expression of glutamine metabolism-related enzymes, as well as glutamine and glutamate consumption by the cells. Therefore, we subsequently assessed whether E7 could possibly affect the sphere-forming capabilities of the C33A cervical cancer cells, in different concentrations of L-glutamine. Our results demonstrated that in the presence of E7, the effects of glutamine starvation on tumor spheres formation diminished, suggesting that E7- and E6E7-expressing cells exhibit less reliance on glutamine (**Figure 16**). Surprisingly, contrary to expectations, these tumor spheres did not displayed upregulation of stemness markers in all glutamine concentrations, as it was observed in non-transduced cells (**Figure 17**). Notably, these unexpected results are supported by a study published by Calvet et al., which demonstrated that tumor spheres can be enriched in CSCs, but this effect varied depending on the specific cell line being used (Calvet et al. 2014). Consequently, a reasonable explanation may be that the process of transduction itself affects the cell line, and subsequently the enrichment of CSCs and the expression of stemness markers. We

were surprised to find that only tumor spheres formed in glutamine starvation demonstrated increased expression of stem cell-related genes in transduced C33A cells. Even through glutamine starvation promotes stemness properties in cancer cells (Prasad et al. 2021), we were also expecting the tumor spheres formed in the 1% and 0.5% L-glutamine concentrations to exhibit upregulation in stemness genes as well. In general, these findings, despite the discordances, are in line with the results of our previous analysis.

Considering the possible effects of E7 in the sphere-forming capabilities of cervical cancer cells in glutamine starvation, we decided to move on to quantify the differences observed in the number and size of the tumor-derived spheroids formed. As expected, significantly less tumor spheres were formed in glutamine starvation (**Figure 18**). Interestingly, we demonstrated that E7-expressing cells formed more tumor spheres, even in the absence of glutamine (**Figure 19**). These observations agree with our previous results, suggesting that glutamine starvation constitutes a limiting factor for the formation of tumor spheres, while in the presence of E7, cells seem to be less sensitive to this limitation. Furthermore, oncogene-expressing cells form tumor spheres that are larger in size in glutamine starvation, compared to non-oncogene-expressing cells, suggest that the presence of the HPV16 oncogenes makes the cells less sensitive to the effects of glutamine starvation (**Figure 21**). However, it is plausible that a number of limitations could have influenced the results obtained. To begin with, there were some difficulties to obtain a high number of tumor spheres, especially in the condition of glutamine starvation. Due to this restriction, we decided to use a smaller sample size, which could potentially affect our results. Another possible source of error might be that we have conducted the tumor spheres quantification manually, which raises the likelihood of human error. Nevertheless, despite some limitations, our data shows that the size data is consistent with the number data, showing that in glutamine deprivation, E7-expressing cells, not only form more tumor spheres, but they are also larger in size.

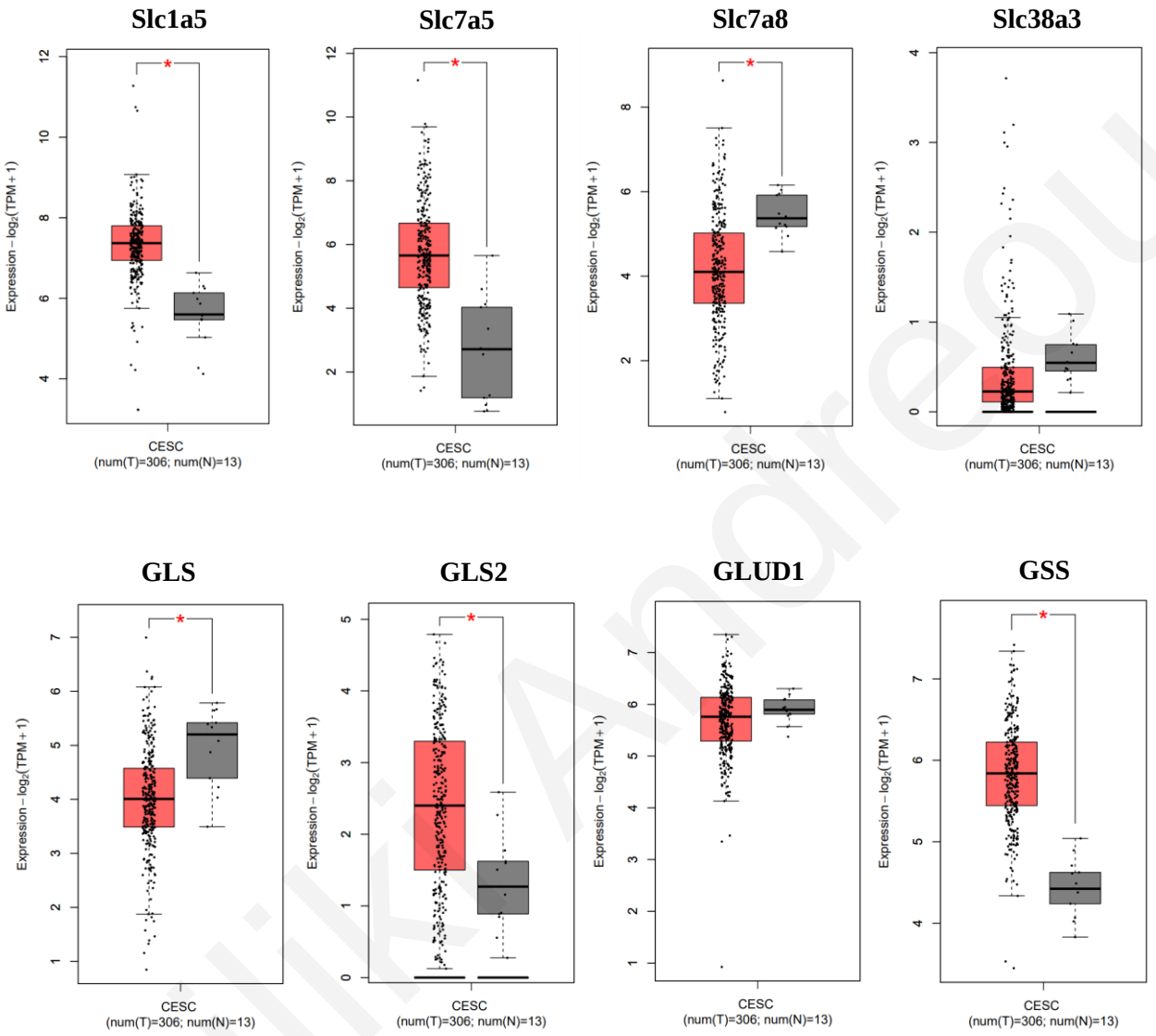


**Figure 22. Key glutamine metabolism-related genes are deregulated in cervical tumors.** Glutamine transporters *Slc1a5* and *Slc7a5*, and the enzymes *GLS2* and *GSS* are overexpressed in cervical squamous cell carcinoma and endocervical adenocarcinoma (TCGA-CESC, n=306) compared to normal cervical tissues (GTEx, n=13) (p-value <0.01). The results shown are in whole based upon data generated by the TCGA Research Network: http://www.cancer.gov/tcga and GTEx database. Data analysis was performed using the GEPIA2 web server: http://gepia2.cancer-pku.cn/#analysis.

## 5. CONCLUSION

In conclusion, our findings provide substantial evidence that the HPV16 oncogenes, E6 and E7, promote metabolic reprogramming, at least in part, by modifying glutamine metabolism in cervical cancer cells. We demonstrated that glutamine transporters and enzymes are upregulated, at least at the transcriptional level, potentially to increase glutamine and glutamate uptake (**Figure 23**). Importantly, these results agree with our analysis using TCGA data, showing that key players of glutamine metabolism are overexpressed in cervical tumors, compared to normal tissues. In addition, we showed that glutamine starvation is a limiting factor for tumor sphere formation, however E7-expressing cells are less sensitive to this limitation. Moreover, we revealed that the presence of E7 not only led to an increase in the number of tumor spheres but also contributed to the growth of larger tumor spheres. Overall, our results are promising, nevertheless additional experiments need to be conducted to draw strong conclusions.

Future work will concentrate on protein analysis to validate whether the transcriptional differences observed for the E7-expressing cells are also true at the protein level. Additionally, to confirm that the effects on the transcription of glutamine metabolism-related enzymes, as well as the observations in the formation of tumor-derived spheroids are E7-specific, HPV positive cervical cancer cell lines can be used to silence E6 and E7 and assess whether a reverse effect is observed. Finally, to check glutamine and glutamate uptake, it would be useful to evaluate, not only the extracellular, but also the intracellular levels of these metabolites. Importantly, we are confident that our study has improved our knowledge and understanding regarding the HPV-induced reprogramming of glutamine metabolism. Moreover, we believe that our findings may have important implications, since an improved comprehension of the biological mechanisms that drive HPV to increase metabolic pathway activity, such as glutaminolysis, can ultimately lead to the development of therapeutic approaches and the detection of biomarkers in HPV-related cancers.

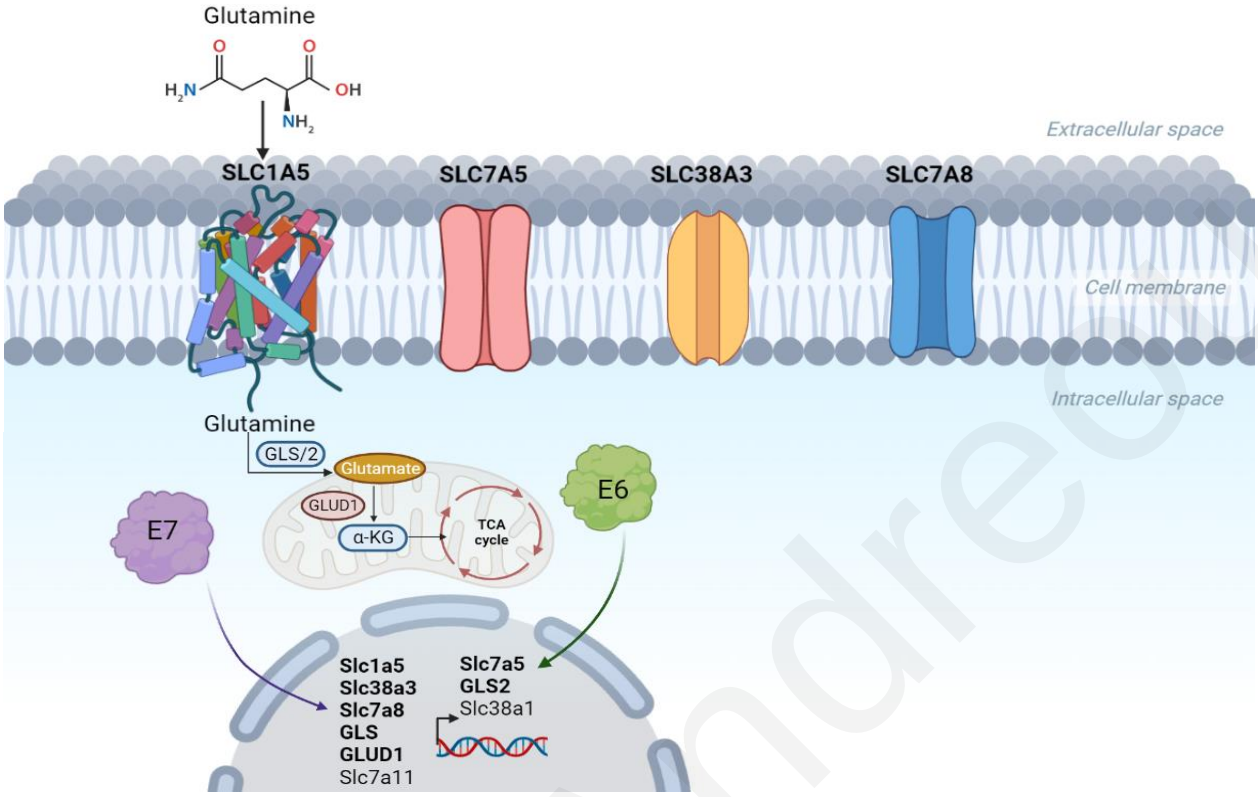


**Figure 23. The HPV16 oncogenes, E6 and E7, modify glutamine metabolism in cervical cancers.** E7 transcriptionally upregulates transporters involved in glutamine metabolism, including *Slc1a5*, *Slc38a3*, *Slc7a8*, *Slc7a5* as well as key glutamine pathway enzymes, *GLS*, *GLS2* and *GLUD1*. E6 only increases the expression levels of *Slc7a5* and *GLS2*. Ortiz-Pedraza et al. (2023), demonstrated that E7 also upregulates *Slc7a11*, while E6 increases the expression of *Slc38a1*. Figure adapted from Ortiz-Pedraza et al. (2023) and it was created with the use of Biorender.com.

## ABBREVIATIONS

| ABBREVIATION | MEANING |
|---|---|
| ATCC | American Type Culture Collection |
| B2M | Beta-2 Microglobulin |
| BC | Breast Cancer |
| cDNA | Complementary Deoxyribonucleic Acid |
| CSCs | Cancer Stem Cells |
| DMEM | Dulbecco's Modified Eagle Medium |
| DNA | Deoxyribonucleic Acid |
| EDTA | Ethylenediaminetetraacetic acid |
| EGF | Epidermal Growth Factor |
| FBS | Fetal Bovine Serum |
| FGF | Fibroblast Growth Factor |
| GAPDH | Glyceraldehyde-3-Phosphate Dehydrogenase |
| GEPIA2 | Gene Expression Profiling Interactive Analysis |
| GLS | Glutaminase |
| GLS2 | Glutaminase 2 |
| GLUD | Glutamate dehydrogenase |
| GSH | Glutathione |
| GSS | Glutathione synthetase |
| GTEx | Genotype-Tissue Expression project |
| HPV | Human Papillomavirus |
| HR-HPV | High-Risk Human Papillomavirus |

| | |
|---|---|
| IDT | Integrated DNA Technologies |
| Klf4 | Kruppel-like Factor 4 |
| LB | Luria Broth |
| MEM | Minimum Essential Medium |
| mRNA | Messenger Ribonucleic Acid |
| $NAD^+$ | Nicotinamide Adenine Dinucleotide |
| NADH | Nicotinamide Adenine Dinucleotide Hydrogen |
| Nono | Non-POU Domain Containing Octamer Binding |
| NSCLC | Non-Small Cell Lung Cancer |
| OC | Ovarian Cancer |
| Oct4 | Octamer-binding Transcription Factor 4 |
| ORF | Open Reading Frame |
| PBS | Phosphate Buffered Saline |
| PCR | Polymerase Chain Reaction |
| pH | Potential Hydrogen |
| pRb | Retinoblastoma Protein |
| RNA | Ribonucleic Acid |
| RPMI | Roswell Park Memorial Institute |
| RT-qPCR | Real-Time quantitative Polymerase Chain Reaction |
| SEM | Standard Error of the Mean |
| Slc1a5 | Solute Carrier 1a5 |
| Slc38a3 | Solute Carrier 38a3 |
| Slc7a5 | Solute Carrier 7a5 |
| Slc7a8 | Solute Carrier 7a8 |

| | |
|---|---|
| Sox2 | SRY-Box Transcription Factor 2 |
| TCA | Tricarboxylic Acid |
| TCGA | The Cancer Genome Atlas |
| TE | Tris-Ethylenediaminetetraacetic acid |
| TNBC | Triple Negative Breast Cancer |
| UV | Ultraviolet |
| WHO | World Health Organization |
| α-KG | α-ketoglutarate |

## BIBLIOGRAPHY

ABD EL-REHIM, D.M., BALL, G., PINDER, S.E., RAKHA, E., PAISH, C., ROBERTSON, J.F.R., MACMILLAN, D., BLAMEY, R.W. and ELLIS, I.O., 2005. High-throughput protein expression analysis using tissue microarray technology of a large well-characterised series identifies biologically distinct classes of breast cancer confirming recent cDNA expression analyses. *International Journal of Cancer*, Sep 1, vol. 116, no. 3, pp. 340-350 ISSN 0020-7136; 0020-7136. DOI 10.1002/ijc.21004.

ARBYN, M., WEIDERPASS, E., BRUNI, L., DE SANJOSÉ, S., SARAIYA, M., FERLAY, J. and BRAY, F., 2020. Estimates of incidence and mortality of cervical cancer in 2018: a worldwide analysis. *The Lancet.Global Health*, 20191204, Feb, vol. 8, no. 2, pp. e191-e203 ISSN 2214-109X; 2214-109X. DOI S2214-109X(19)30482-6 [pii].

ARIZMENDI-IZAZAGA, A., NAVARRO-TITO, N., JIMÉNEZ-WENCES, H., MENDOZA-CATALÁN, M.A., MARTÍNEZ-CARRILLO, D.N., ZACAPALA-GÓMEZ, A.E., OLEA-FLORES, M., DIRCIO-MALDONADO, R., TORRES-ROJAS, F.I., SOTO-FLORES, D.G., ILLADES-AGUIAR, B. and ORTIZ-ORTIZ, J., 2021. Metabolic Reprogramming in Cancer: Role of HPV 16 Variants. *Pathogens (Basel, Switzerland)*, 20210316, Mar 16, vol. 10, no. 3, pp. 347. doi: 10.3390/pathogens10030347 ISSN 2076-0817; 2076-0817; 2076-0817. DOI 10.3390/pathogens10030347.

BHUTIA, Y.D. and GANAPATHY, V., 2016. Glutamine transporters in mammalian cells and their functions in physiology and cancer. *Biochimica Et Biophysica Acta*, 20151224, Oct, vol. 1863, no. 10, pp. 2531-2539 ISSN 0006-3002; 0006-3002. DOI 10.1016/j.bbamcr.2015.12.017.

BOUVARD, V., BAAN, R., STRAIF, K., GROSSE, Y., SECRETAN, B., EL GHISSASSI, F., BENBRAHIM-TALLAA, L., GUHA, N., FREEMAN, C., GALICHET, L., COGLIANO, V. and WHO International Agency for Research on Cancer Monograph Working Group, 2009. A review of human carcinogens--Part B: biological agents. *The Lancet.Oncology*,

Apr, vol. 10, no. 4, pp. 321-322 ISSN 1474-5488; 1470-2045. DOI 10.1016/s1470-2045(09)70096-8 [doi].

BRAY, F., FERLAY, J., SOERJOMATARAM, I., SIEGEL, R.L., TORRE, L.A. and JEMAL, A., 2018. Global cancer statistics 2018: GLOBOCAN estimates of incidence and mortality worldwide for 36 cancers in 185 countries. *CA: A Cancer Journal for Clinicians*, 20180912, Nov, vol. 68, no. 6, pp. 394-424 ISSN 1542-4863; 0007-9235. DOI 10.3322/caac.21492.

CALVET, C.Y., ANDRÉ, F.M. and MIR, L.M., 2014. The culture of cancer cell lines as tumorspheres does not systematically result in cancer stem cell enrichment. *PLoS One*, vol. 9, no. 2, pp. e89644.

CHIODI, I., PICCO, G., MARTINO, C. and MONDELLO, C., 2019. Cellular response to glutamine and/or glucose deprivation in in vitro transformed human fibroblasts. *Oncology Reports*, vol. 41, no. 6, pp. 3555-3564.

CURTIS, C., SHAH, S.P., CHIN, S., TURASHVILI, G., RUEDA, O.M., DUNNING, M.J., SPEED, D., LYNCH, A.G., SAMARAJIWA, S., YUAN, Y., GRÄF, S., HA, G., HAFFARI, G., BASHASHATI, A., RUSSELL, R., MCKINNEY, S., METABRIC Group, LANGERØD, A., GREEN, A., PROVENZANO, E., WISHART, G., PINDER, S., WATSON, P., MARKOWETZ, F., MURPHY, L., ELLIS, I., PURUSHOTHAM, A., BØRRESEN-DALE, A., BRENTON, J.D., TAVARÉ, S., CALDAS, C. and APARICIO, S., 2012. The genomic and transcriptomic architecture of 2,000 breast tumours reveals novel subgroups. *Nature*, 20120418, Apr 18, vol. 486, no. 7403, pp. 346-352 ISSN 1476-4687; 0028-0836; 0028-0836. DOI 10.1038/nature10983.

DEMAS, D.M., DEMO, S., FALLAH, Y., CLARKE, R., NEPHEW, K.P., ALTHOUSE, S., SANDUSKY, G., HE, W. and SHAJAHAN-HAQ, A.N., 2019. Glutamine Metabolism Drives Growth in Advanced Hormone Receptor Positive Breast Cancer. *Frontiers in Oncology*, 20190802, Aug 2, vol. 9, pp. 686 ISSN 2234-943X; 2234-943X; 2234-943X. DOI 10.3389/fonc.2019.00686.

DIAS, M.M., ADAMOSKI, D., DOS REIS, L.M., ASCENÇÃO, C.F.R., de Oliveira, Krishina R S, MAFRA, A.C.P., da Silva Bastos, Alliny Cristiny, QUINTERO, M., DE G CASSAGO, C., FERREIRA, I.M., FIDELIS, C.H.V., ROCCO, S.A., BAJGELMAN, M.C., STINE, Z., BERINDAN-NEAGOE, I., CALIN, G.A., AMBROSIO, A.L.B. and DIAS, S.M.G., 2020. GLS2 is protumorigenic in breast cancers. *Oncogene*, 20190920, Jan, vol. 39, no. 3, pp. 690-702 ISSN 1476-5594; 0950-9232. DOI 10.1038/s41388-019-1007-z.

EKICI, S., RISK, B.B., NEILL, S.G., SHU, H. and FLEISCHER, C.C., 2020. Characterization of dysregulated glutamine metabolism in human glioma tissue with (1)H NMR. *Scientific Reports*, 20201124, Nov 24, vol. 10, no. 1, pp. 20435-020-76982-7 ISSN 2045-2322; 2045-2322. DOI 10.1038/s41598-020-76982-7.

EL ANSARI, R., ALFARSI, L., CRAZE, M.L., MASISI, B.K., ELLIS, I.O., RAKHA, E.A. and GREEN, A.R., 2020. The solute carrier SLC7A8 is a marker of favourable prognosis in ER-positive low proliferative invasive breast cancer. *Breast Cancer Research and Treatment*, 20200321, May, vol. 181, no. 1, pp. 1-12 ISSN 1573-7217; 0167-6806; 0167-6806. DOI 10.1007/s10549-020-05586-6.

ELIA, I. and HAIGIS, M.C., 2021. Metabolites and the tumour microenvironment: from cellular mechanisms to systemic metabolism. *Nature Metabolism*, 20210104, Jan, vol. 3, no. 1, pp. 21-32 ISSN 2522-5812; 2522-5812. DOI 10.1038/s42255-020-00317-z.

ESTÊVÃO, D., COSTA, N.R., GIL DA COSTA, R.M. and MEDEIROS, R., 2019. Hallmarks of HPV carcinogenesis: The role of E6, E7 and E5 oncoproteins in cellular malignancy. *Biochimica Et Biophysica Acta.Gene Regulatory Mechanisms*, 20190129, Feb, vol. 1862, no. 2, pp. 153-162 ISSN 1876-4320; 1874-9399. DOI S1874-9399(18)30520-0 [pii].

GHITTONI, R., ACCARDI, R., CHIOCCA, S. and TOMMASINO, M., 2015. Role of human papillomaviruses in carcinogenesis. *Ecancermedicalscience*, 20150429, Apr 29, vol. 9, pp. 526 ISSN 1754-6605; 1754-6605; 1754-6605. DOI 10.3332/ecancer.2015.526 [doi].

GUPTA, S., KUMAR, P. and DAS, B.C., 2018. HPV: Molecular pathways and targets. *Current Problems in Cancer*, 20180405, Mar-Apr, vol. 42, no. 2, pp. 161-174 ISSN 1535-6345; 0147-0272. DOI S0147-0272(18)30077-1 [pii].

HANAHAN, D. and WEINBERG, R.A., 2011. Hallmarks of cancer: the next generation. *Cell*, Mar 4, vol. 144, no. 5, pp. 646-674 ISSN 1097-4172; 0092-8674. DOI 10.1016/j.cell.2011.02.013.

HANAHAN, D. and WEINBERG, R.A., 2011. Hallmarks of cancer: the next generation. *Cell*, Mar 4, vol. 144, no. 5, pp. 646-674 ISSN 1097-4172; 0092-8674. DOI 10.1016/j.cell.2011.02.013 [doi].

HWANG, S.G., LEE, D., KIM, J., SEO, T. and CHOE, J., 2002. Human papillomavirus type 16 E7 binds to E2F1 and activates E2F1-driven transcription in a retinoblastoma protein-independent manner. *The Journal of Biological Chemistry*, 20011116, Jan 25, vol. 277, no. 4, pp. 2923-2930 ISSN 0021-9258; 0021-9258. DOI S0021-9258(20)87749-7 [pii].

JIN, L., ALESI, G.N. and KANG, S., 2016. Glutaminolysis as a target for cancer therapy. *Oncogene*, 20151123, Jul 14, vol. 35, no. 28, pp. 3619-3625 ISSN 1476-5594; 0950-9232; 0950-9232. DOI 10.1038/onc.2015.447.

KAIRA, K., ORIUCHI, N., IMAI, H., SHIMIZU, K., YANAGITANI, N., SUNAGA, N., HISADA, T., ISHIZUKA, T., KANAI, Y., ENDOU, H., NAKAJIMA, T. and MORI, M., 2009. L-type amino acid transporter 1 (LAT1) is frequently expressed in thymic carcinomas but is absent in thymomas. *Journal of Surgical Oncology*, Jun 1, vol. 99, no. 7, pp. 433-438 ISSN 1096-9098; 0022-4790. DOI 10.1002/jso.21277.

KANAI, Y., 2022. Amino acid transporter LAT1 (SLC7A5) as a molecular target for cancer diagnosis and therapeutics. *Pharmacology & Therapeutics*, 20210812, Feb, vol. 230, pp. 107964 ISSN 1879-016X; 0163-7258. DOI 10.1016/j.pharmthera.2021.107964.

KIM, A.D., ZHANG, R., HAN, X., KANG, K.A., PIAO, M.J., MAENG, Y.H., CHANG, W.Y. and HYUN, J.W., 2015. Involvement of glutathione and glutathione metabolizing enzymes

in human colorectal cancer cell lines and tissues. *Molecular Medicine Reports*, vol. 12, no. 3, pp. 4314-4319.

KIM, M.H. and KIM, H., 2013. Oncogenes and tumor suppressors regulate glutamine metabolism in cancer cells. *Journal of Cancer Prevention*, Sep, vol. 18, no. 3, pp. 221-226 ISSN 2288-3649; 2288-3657; 2288-3649. DOI 10.15430/jcp.2013.18.3.221.

LE, A., 2021. *The heterogeneity of cancer metabolism.* Springer Nature.

LI, B. and SUI, L., 2021. Metabolic reprogramming in cervical cancer and metabolomics perspectives. *Nutrition & Metabolism*, 20211019, Oct 19, vol. 18, no. 1, pp. 93-021-00615-7 ISSN 1743-7075; 1743-7075; 1743-7075. DOI 10.1186/s12986-021-00615-7.

LI, T. and LE, A., 2018. Glutamine Metabolism in Cancer. *Advances in Experimental Medicine and Biology*, vol. 1063, pp. 13-32 ISSN 0065-2598; 0065-2598. DOI 10.1007/978-3-319-77736-8_2.

LI, Y., WANG, W., WU, X., LING, S., MA, Y. and HUANG, P., 2021. SLC7A5 serves as a prognostic factor of breast cancer and promotes cell proliferation through activating AKT/mTORC1 signaling pathway. *Annals of Translational Medicine*, May, vol. 9, no. 10, pp. 892-21-2247 ISSN 2305-5839; 2305-5847; 2305-5839. DOI 10.21037/atm-21-2247.

LIU, R., HONG, R., WANG, Y., GONG, Y., YEERKEN, D., YANG, D., LI, J., FAN, J., CHEN, J., ZHANG, W. and ZHAN, Q., 2020. Defect of SLC38A3 promotes epithelial-mesenchymal transition and predicts poor prognosis in esophageal squamous cell carcinoma. *Chinese Journal of Cancer Research = Chung-Kuo Yen Cheng Yen Chiu*, Oct 31, vol. 32, no. 5, pp. 547-563 ISSN 1000-9604; 1993-0631; 1000-9604. DOI 10.21147/j.issn.1000-9604.2020.05.01.

MARTÍNEZ-REYES, I. and CHANDEL, N.S., 2021. Cancer metabolism: looking forward. *Nature Reviews.Cancer*, 20210716, Oct, vol. 21, no. 10, pp. 669-680 ISSN 1474-1768; 1474-175X. DOI 10.1038/s41568-021-00378-6.

MARTINEZ-ZAPIEN, D., RUIZ, F.X., POIRSON, J., MITSCHLER, A., RAMIREZ, J., FORSTER, A., COUSIDO-SIAH, A., MASSON, M., VANDE POL, S., PODJARNY, A., TRAVÉ, G. and ZANIER, K., 2016. Structure of the E6/E6AP/p53 complex required for HPV-mediated degradation of p53. *Nature*, 20160120, Jan 28, vol. 529, no. 7587, pp. 541-545 ISSN 1476-4687; 0028-0836; 0028-0836. DOI 10.1038/nature16481 [doi].

MATÉS, J.M., CAMPOS-SANDOVAL, J.A., SANTOS-JIMÉNEZ, J.d.L. and MÁRQUEZ, J., 2019. Dysregulation of glutaminase and glutamine synthetase in cancer. *Cancer Letters*, 20190928, Dec 28, vol. 467, pp. 29-39 ISSN 1872-7980; 0304-3835. DOI 10.1016/j.canlet.2019.09.011.

MITTAL, S. and BANKS, L., 2017. Molecular mechanisms underlying human papillomavirus E6 and E7 oncoprotein-induced cell transformation. *Mutation Research.Reviews in Mutation Research*, 20160805, Apr-Jun, vol. 772, pp. 23-35 ISSN 1388-2139; 1383-5742. DOI 10.1016/j.mrrev.2016.08.001.

MOODY, C.A. and LAIMINS, L.A., 2010. Human papillomavirus oncoproteins: pathways to transformation. *Nature Reviews.Cancer*, 20100701, Aug, vol. 10, no. 8, pp. 550-560 ISSN 1474-1768; 1474-175X. DOI 10.1038/nrc2886 [doi].

NATIONAL HEALTH SYSTEM, N., 2021.2 September 2021, Available from: https://www.nhs.uk/conditions/cervical-cancer/.

National Institute of Health, NIH., 2022.October 13, 2022, Available from: https://www.cancer.gov/types/cervical.

NI, R., LI, Z., LI, L., PENG, D., MING, Y., LI, L. and LIU, Y., 2023. Rethinking glutamine metabolism and the regulation of glutamine addiction by oncogenes in cancer. *Frontiers in Oncology*, 20230307, Mar 7, vol. 13, pp. 1143798 ISSN 2234-943X; 2234-943X; 2234-943X. DOI 10.3389/fonc.2023.1143798.

ORTIZ-PEDRAZA, Y., MUÑOZ-BELLO, J.O., RAMOS-CHÁVEZ, L.A., MARTÍNEZ-RAMÍREZ, I., OLMEDO-NIEVA, L., MANZO-MERINO, J., LÓPEZ-SAAVEDRA, A.,

PÉREZ-DE LA CRUZ, V. and LIZANO, M., 2023. HPV16 E6 and E7 Oncoproteins Stimulate the Glutamine Pathway Maintaining Cell Proliferation in a SNAT1-Dependent Fashion. *Viruses*, vol. 15, no. 2, pp. 324.

PAPPA, K.I., DASKALAKIS, G. and ANAGNOU, N.P., 2021. Metabolic rewiring is associated with HPV-specific profiles in cervical cancer cell lines. *Scientific Reports*, 20210906, Sep 6, vol. 11, no. 1, pp. 17718-021-96038-8 ISSN 2045-2322; 2045-2322. DOI 10.1038/s41598-021-96038-8.

PASCALE, R.M., CALVISI, D.F., SIMILE, M.M., FEO, C.F. and FEO, F., 2020. The Warburg Effect 97 Years after Its Discovery. *Cancers*, 20200930, Sep 30, vol. 12, no. 10, pp. 2819. doi: 10.3390/cancers12102819 ISSN 2072-6694; 2072-6694; 2072-6694. DOI 10.3390/cancers12102819.

PAVLOVA, N.N. and THOMPSON, C.B., 2016. The Emerging Hallmarks of Cancer Metabolism. *Cell Metabolism*, Jan 12, vol. 23, no. 1, pp. 27-47 ISSN 1932-7420; 1550-4131; 1550-4131. DOI 10.1016/j.cmet.2015.12.006.

PRASAD, P., GHOSH, S. and ROY, S.S., 2021. Glutamine deficiency promotes stemness and chemoresistance in tumor cells through DRP1-induced mitochondrial fragmentation. *Cellular and Molecular Life Sciences : CMLS*, 20210424, May, vol. 78, no. 10, pp. 4821-4845 ISSN 1420-9071; 1420-682X. DOI 10.1007/s00018-021-03818-6.

QIE, S., LIANG, D., YIN, C., GU, W., MENG, M., WANG, C. and SANG, N., 2012. Glutamine depletion and glucose depletion trigger growth inhibition via distinctive gene expression reprogramming. *Cell Cycle (Georgetown, Tex.)*, 20120830, Oct 1, vol. 11, no. 19, pp. 3679-3690 ISSN 1551-4005; 1538-4101; 1551-4005. DOI 10.4161/cc.21944.

REYNOLDS, M.R., LANE, A.N., ROBERTSON, B., KEMP, S., LIU, Y., HILL, B.G., DEAN, D.C. and CLEM, B.F., 2014. Control of glutamine metabolism by the tumor suppressor Rb. *Oncogene*, 20130128, Jan 30, vol. 33, no. 5, pp. 556-566 ISSN 1476-5594; 0950-9232; 0950-9232. DOI 10.1038/onc.2012.635.

SCHEFFNER, M., WERNESS, B.A., HUIBREGTSE, J.M., LEVINE, A.J. and HOWLEY, P.M., 1990. The E6 oncoprotein encoded by human papillomavirus types 16 and 18 promotes the degradation of p53. *Cell*, Dec 21, vol. 63, no. 6, pp. 1129-1136 ISSN 0092-8674; 0092-8674. DOI 0092-8674(90)90409-8 [pii].

SCHILIRO, C. and FIRESTEIN, B.L., 2021. Mechanisms of Metabolic Reprogramming in Cancer Cells Supporting Enhanced Growth and Proliferation. *Cells*, 20210429, Apr 29, vol. 10, no. 5, pp. 1056. doi: 10.3390/cells10051056 ISSN 2073-4409; 2073-4409. DOI 10.3390/cells10051056.

SON, J., LYSSIOTIS, C.A., YING, H., WANG, X., HUA, S., LIGORIO, M., PERERA, R.M., FERRONE, C.R., MULLARKY, E., SHYH-CHANG, N., KANG, Y., FLEMING, J.B., BARDEESY, N., ASARA, J.M., HAIGIS, M.C., DEPINHO, R.A., CANTLEY, L.C. and KIMMELMAN, A.C., 2013. Glutamine supports pancreatic cancer growth through a KRAS-regulated metabolic pathway. *Nature*, 20130327, Apr 4, vol. 496, no. 7443, pp. 101-105 ISSN 1476-4687; 0028-0836; 0028-0836. DOI 10.1038/nature12040.

TAN, Z., TRESSLER, C.M., SONKAR, K. and GLUNDE, K., 2021. Abstract LB207: Glutamine transporter SLC38A3 promotes breast cancer migration via GSK3beta/beta-catenin/EMT pathway. Cancer Research, vol. 81, no. 13_Supplement, pp. LB207-LB207.

TAYLOR, S.R., FALCONE, J.N., CANTLEY, L.C. and GONCALVES, M.D., 2022. Developing dietary interventions as therapy for cancer. *Nature Reviews Cancer*, vol. 22, no. 8, pp. 452-466.

TIMMERMAN, L.A., HOLTON, T., YUNEVA, M., LOUIE, R.J., PADRÓ, M., DAEMEN, A., HU, M., CHAN, D.A., ETHIER, S.P., van 't Veer, Laura J, POLYAK, K., MCCORMICK, F. and GRAY, J.W., 2013. Glutamine sensitivity analysis identifies the xCT antiporter as a common triple-negative breast tumor therapeutic target. *Cancer Cell*, 20131003, Oct 14, vol. 24, no. 4, pp. 450-465 ISSN 1878-3686; 1535-6108; 1535-6108. DOI 10.1016/j.ccr.2013.08.020.

TIRINO, V., DESIDERIO, V., PAINO, F., DE ROSA, A., PAPACCIO, F., LA NOCE, M., LAINO, L., DE FRANCESCO, F. and PAPACCIO, G., 2013. Cancer stem cells in solid tumors: an overview and new approaches for their isolation and characterization. *FASEB Journal : Official Publication of the Federation of American Societies for Experimental Biology*, 20120928, Jan, vol. 27, no. 1, pp. 13-24 ISSN 1530-6860; 0892-6638. DOI 10.1096/fj.12-218222.

WANG, Q. and HOLST, J., 2015. L-type amino acid transport and cancer: targeting the mTORC1 pathway to inhibit neoplasia. *American Journal of Cancer Research*, 20150315, Mar 15, vol. 5, no. 4, pp. 1281-1294 ISSN 2156-6976; 2156-6976; 2156-6976.

WANG, Y., FU, L., CUI, M., WANG, Y., XU, Y., LI, M. and MI, J., 2017. Amino acid transporter SLC38A3 promotes metastasis of non-small cell lung cancer cells by activating PDK1. *Cancer Letters*, 20170213, May 1, vol. 393, pp. 8-15 ISSN 1872-7980; 0304-3835. DOI 10.1016/j.canlet.2017.01.036.

WARBURG, O., WIND, F. and NEGELEIN, E., 1927. The Metabolism of Tumors in the Body. *The Journal of General Physiology*, Mar 7, vol. 8, no. 6, pp. 519-530 ISSN 0022-1295; 1540-7748; 0022-1295. DOI 10.1085/jgp.8.6.519.

WARD, P.S. and THOMPSON, C.B., 2012. Metabolic reprogramming: a cancer hallmark even warburg did not anticipate. *Cancer Cell*, Mar 20, vol. 21, no. 3, pp. 297-308 ISSN 1878-3686; 1535-6108; 1535-6108. DOI 10.1016/j.ccr.2012.02.014.

WISE, D.R., DEBERARDINIS, R.J., MANCUSO, A., SAYED, N., ZHANG, X., PFEIFFER, H.K., NISSIM, I., DAIKHIN, E., YUDKOFF, M., MCMAHON, S.B. and THOMPSON, C.B., 2008. Myc regulates a transcriptional program that stimulates mitochondrial glutaminolysis and leads to glutamine addiction. *Proceedings of the National Academy of Sciences of the United States of America*, 20081124, Dec 2, vol. 105, no. 48, pp. 18782-18787 ISSN 1091-6490; 0027-8424; 0027-8424. DOI 10.1073/pnas.0810199105.

WISE, D.R. and THOMPSON, C.B., 2010. Glutamine addiction: a new therapeutic target in cancer. *Trends in Biochemical Sciences*, Aug, vol. 35, no. 8, pp. 427-433 ISSN 0968-0004; 0968-0004. DOI 10.1016/j.tibs.2010.05.003.

WORLD HEALTH ORGANIZATION, W., 2022a.February 22, 2022, Available from: https://www.who.int/news-room/fact-sheets/detail/cervical-cancer#:~:text=Cervical%20cancer%20is%20the%20fourth,%2Dincome%20countries%20(1).

WORLD HEALTH ORGANIZATION, W., 2022b.April 11, 2022, Available from: https://www.who.int/news/item/11-04-2022-one-dose-human-papillomavirus-(hpv)-vaccine-offers-solid-protection-against-cervical-cancer.

YANG, L., VENNETI, S. and NAGRATH, D., 2017. Glutaminolysis: A Hallmark of Cancer Metabolism. *Annual Review of Biomedical Engineering*, 20170308, Jun 21, vol. 19, pp. 163-194 ISSN 1545-4274; 1523-9829. DOI 10.1146/annurev-bioeng-071516-044546.

YANG, R., KLIMENTOVÁ, J., GÖCKEL-KRZIKALLA, E., LY, R., GMELIN, N., HOTZ-WAGENBLATT, A., ŘEHULKOVÁ, H., STULÍK, J., RÖSL, F. and NIEBLER, M., 2019. Combined Transcriptome and Proteome Analysis of Immortalized Human Keratinocytes Expressing Human Papillomavirus 16 (HPV16) Oncogenes Reveals Novel Key Factors and Networks in HPV-Induced Carcinogenesis. *mSphere*, 20190327, Mar 27, vol. 4, no. 2, pp. e00129-19. doi: 10.1128/mSphere.00129-19 ISSN 2379-5042; 2379-5042. DOI 10.1128/mSphere.00129-19 [doi].

YOO, H.C., YU, Y.C., SUNG, Y. and HAN, J.M., 2020. Glutamine reliance in cell metabolism. *Experimental & Molecular Medicine*, 20200917, Sep, vol. 52, no. 9, pp. 1496-1516 ISSN 2092-6413; 1226-3613; 1226-3613. DOI 10.1038/s12276-020-00504-8.

YU, L., MAJERCIAK, V. and ZHENG, Z., 2022. HPV16 and HPV18 Genome Structure, Expression, and Post-Transcriptional Regulation. *International Journal of Molecular Sciences*, 20220429, Apr 29, vol. 23, no. 9, pp. 4943. doi: 10.3390/ijms23094943 ISSN 1422-0067; 1422-0067. DOI 10.3390/ijms23094943.

YUAN, L., SHENG, X., WILLSON, A.K., ROQUE, D.R., STINE, J.E., GUO, H., JONES, H.M., ZHOU, C. and BAE-JUMP, V.L., 2015. Glutamine promotes ovarian cancer cell proliferation through the mTOR/S6 pathway. *Endocrine-Related Cancer*, 20150604, Aug, vol. 22, no. 4, pp. 577-591 ISSN 1479-6821; 1351-0088; 1351-0088. DOI 10.1530/ERC-15-0192.

YUNEVA, M., ZAMBONI, N., OEFNER, P., SACHIDANANDAM, R. and LAZEBNIK, Y., 2007. Deficiency in glutamine but not glucose induces MYC-dependent apoptosis in human cells. *The Journal of Cell Biology*, vol. 178, no. 1, pp. 93-105.

ZHANG, J., PAVLOVA, N.N. and THOMPSON, C.B., 2017. Cancer cell metabolism: the essential role of the nonessential amino acid, glutamine. *The EMBO Journal*, 20170418, May 15, vol. 36, no. 10, pp. 1302-1315 ISSN 1460-2075; 0261-4189; 0261-4189. DOI 10.15252/embj.201696151.

ZHANG, J., WANG, G., MAO, Q., LI, S., XIONG, W., LIN, Y. and GE, J., 2016. Glutamate dehydrogenase (GDH) regulates bioenergetics and redox homeostasis in human glioma. *Oncotarget*, vol. 5.

ZHANG, S., XU, H., ZHANG, L. and QIAO, Y., 2020. Cervical cancer: Epidemiology, risk factors and screening. *Chinese Journal of Cancer Research = Chung-Kuo Yen Cheng Yen Chiu*, Dec 31, vol. 32, no. 6, pp. 720-728 ISSN 1000-9604; 1993-0631; 1000-9604. DOI 10.21147/j.issn.1000-9604.2020.06.05.

# APPENDICES

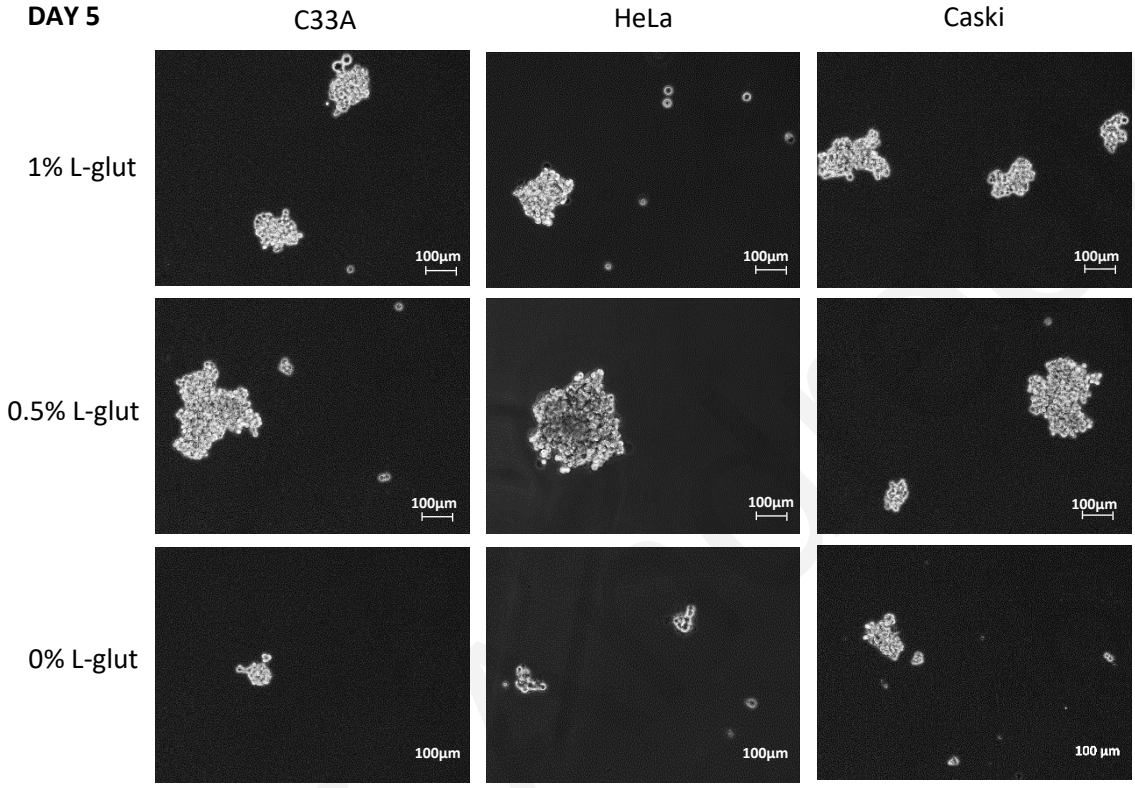


**Appendix 1. Tumor spheres cannot be efficiently formed in glutamine starvation.** Representative phase-contrast images of the tumor spheres formed from cervical cancer cells C33A, HeLa and CaSki, in different concentrations of L-glutamine (1%, 0.5% and 0% L-glutamine). The images were taken on day 5 of the tumor spheres assay, using the 10x lens of the Axio camera (Zeiss Axio Observer.A1) and are representative of three independent experiments. Scale bars, 100µm.

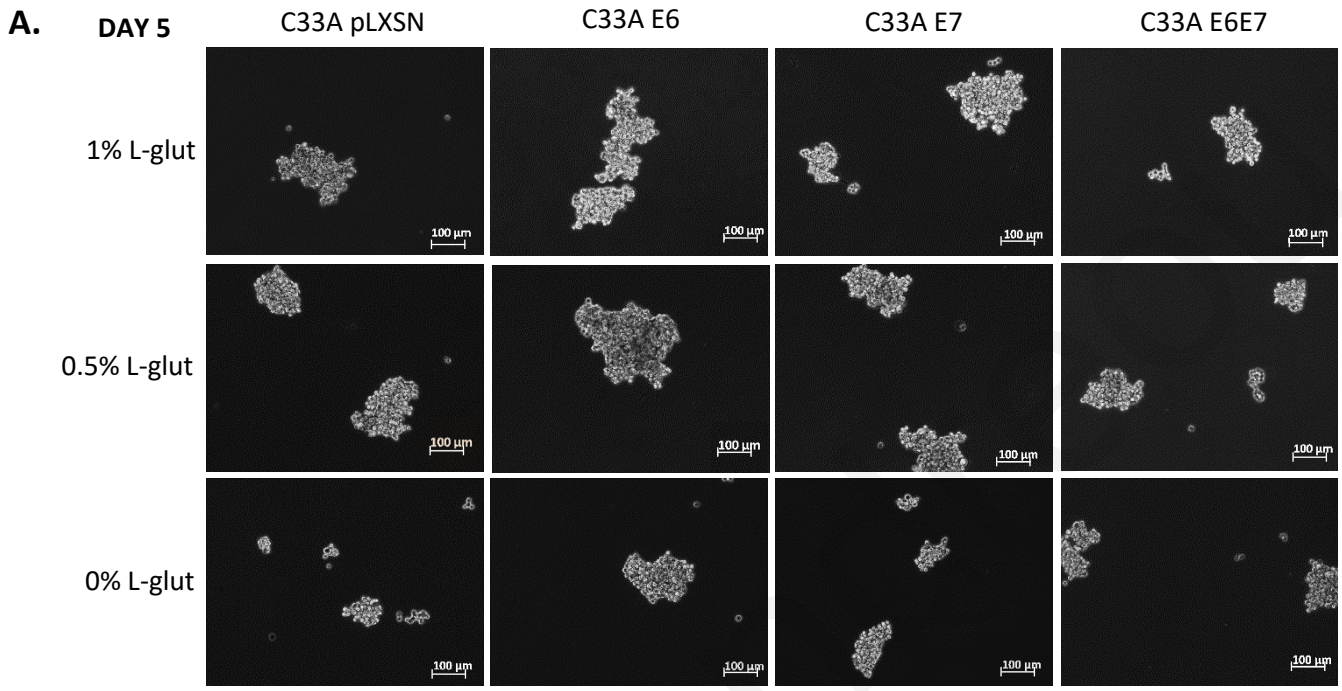
A.
DAY 5
C33A pLXSN
C33A E6
C33A E7
C33A E6E7
1% L-glut
0.5% L-glut
0% L-glut
100 µm

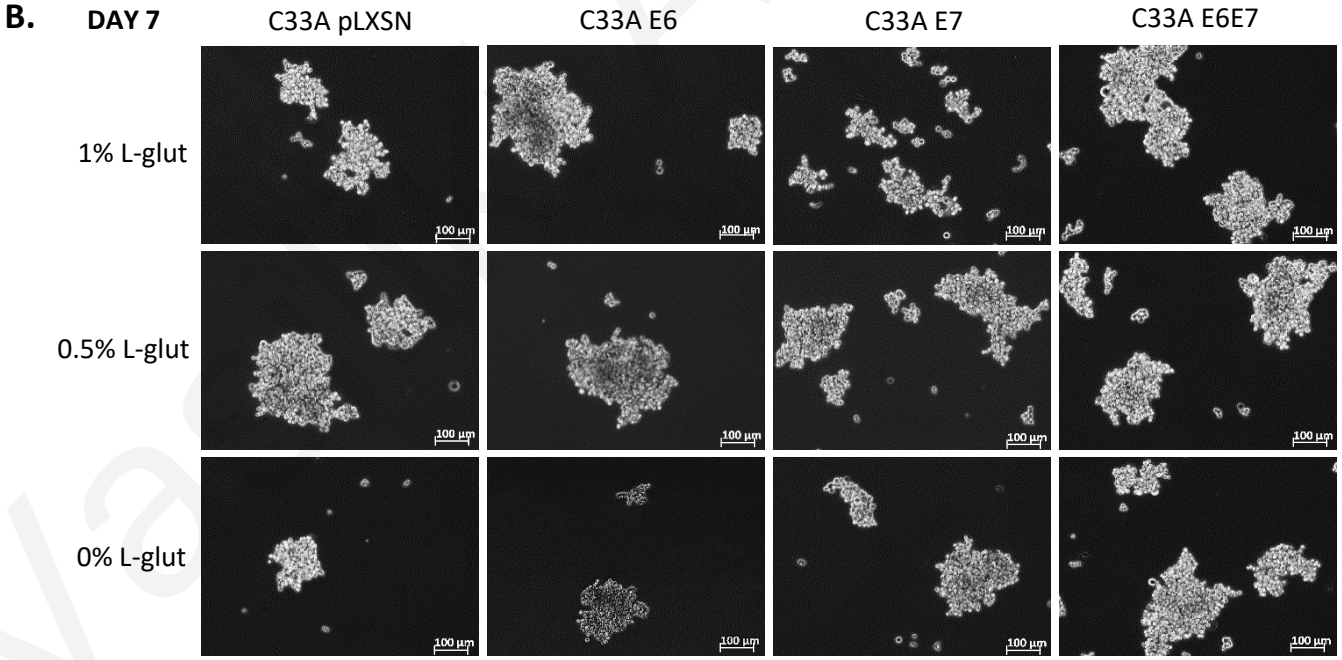
B.
DAY 7
C33A pLXSN
C33A E6
C33A E7
C33A E6E7
1% L-glut
0.5% L-glut
0% L-glut
100 µm

**Appendix 2.**

Representative phase-contrast images of the tumor spheres formed from HPV-negative cervical cancer cells, C33A, expressing the viral oncogenes (HPV16 E6/E7/E6E7), in different concentrations of L-glutamine (1%, 0.5% and 0% L-glutamine). The images were taken on **(A)** day 5 and **(B)** day 7 of the tumor spheres assay, using the 10x lens of the Axio camera (Zeiss Axio Observer.A1) and are representative of three independent experiments. Scale bars, 100μm.

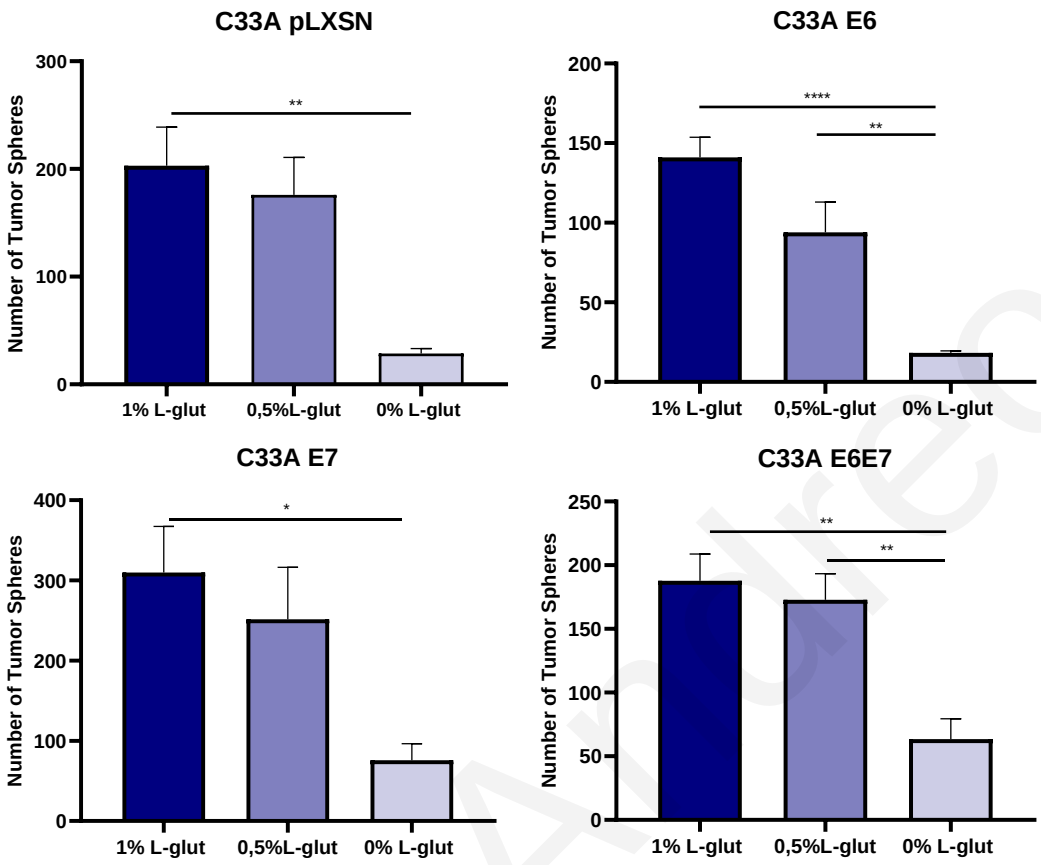


**Appendix 3. Less tumor spheres are formed in the absence of L-glutamine.** Absolute numbers of tumor spheres formed using the different cell lines C33A pLXSN, C33A E6, C33A E7 and C33A E6E7, in different concentrations of L-glutamine (1%, 0.5% and 0% L-glutamine) were plotted, using the GraphPad Prism software 8.0.1. Data presented as mean ± SEM of three biological replicates and are representative of three independent experiments. Statistical significance was evaluated using the one-way ANOVA statistical test. P <0.05 was considered statistically significant. (ns = non-significant, *p<0.05, **p<0.01, ***p<0.001, ****p<0.0001).

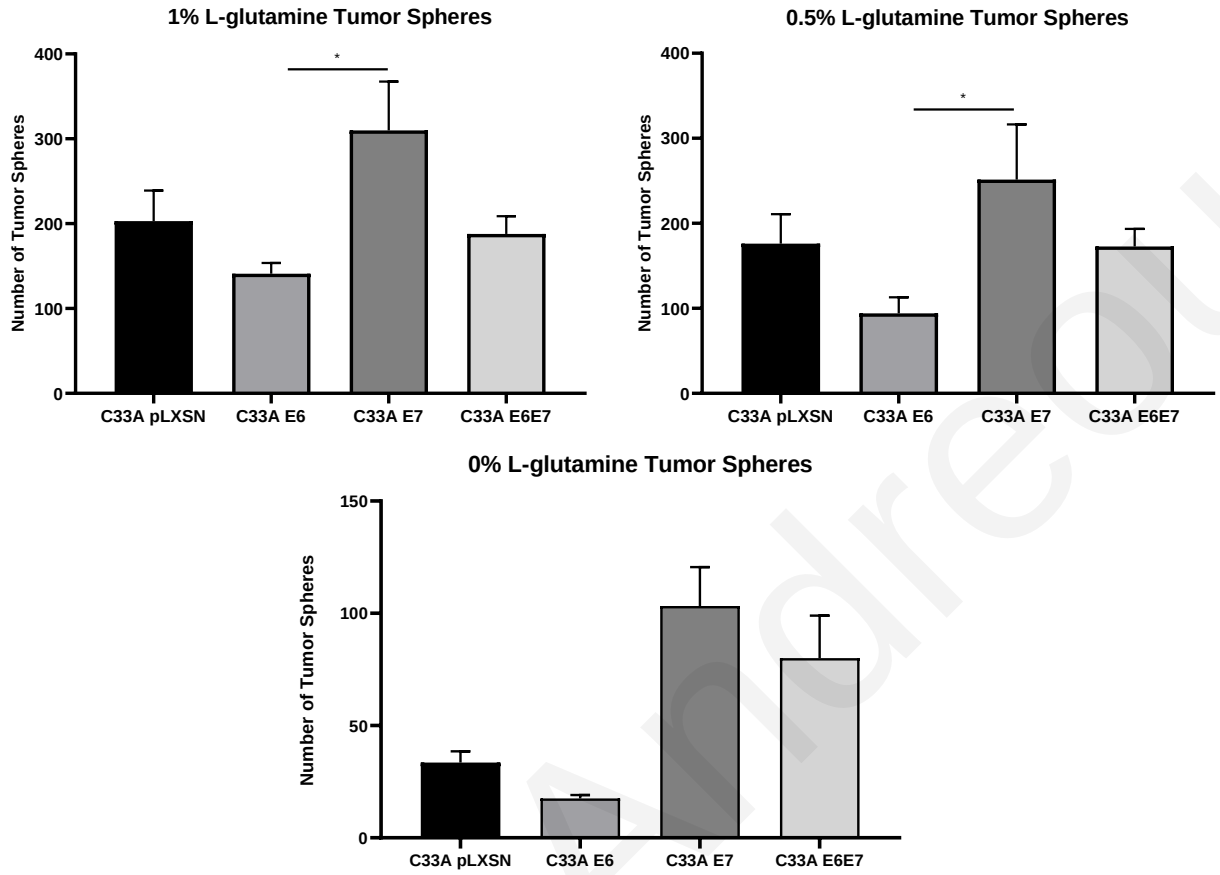


**Appendix 4. E7-expressing cells form more tumor spheres in all concentrations of L-glutamine, even in glutamine starvation.** Absolute numbers of tumor spheres formed using the different cell lines C33A pLXSN, C33A E6, C33A E7 and C33A E6E7, in different concentrations of L-glutamine (1%, 0.5% and 0% L-glutamine) were plotted, using the GraphPad Prism software 8.0.1. Data presented as mean ± SEM of three biological replicates and are representative of three independent experiments. Statistical significance was evaluated using the one-way ANOVA statistical test. P <0.05 was considered statistically significant. (ns = non-significant, *p<0.05, **p<0.01, ***p<0.001, ****p<0.0001).